Journal of Medicinal Chemistry

Article

pubs.acs.org/jmc

# Identification and Characterization of Von Hippel-Lindau-Recruiting Proteolysis Targeting Chimeras (PROTACs) of TANK-Binding Kinase 1

Andrew P. Crew,*[,†] Kanak Raina,[†] Hanqing Dong,[†] Yimin Qian,[†] Jing Wang,[†] Dominico Vigil,[†,∥] Yevgeniy V. Serebrenik,[‡] Brian D. Hamman,[†] Alicia Morgan,[†] Caterina Ferraro,[†] Kam Siu,[†] Taavi K. Neklesa,[†] James D. Winkler,[†] Kevin G. Coleman,[†] and Craig M. Crews*[,‡,§]

[†]Arvinas LLC, 5 Science Park, New Haven, Connecticut 06511, United States

[‡]Department of Molecular, Cell and Developmental Biology, [§]Departments of Chemistry and Pharmacology, Yale University, New Haven, Connecticut 06511, United States

Supporting Information

**ABSTRACT:** Proteolysis targeting chimeras (PROTACs) are bifunctional molecules that recruit an E3 ligase to a target protein to facilitate ubiquitination and subsequent degradation of that protein. While the field of targeted degraders is still relatively young, the potential for this modality to become a differentiated and therapeutic reality is strong, such that both academic and pharmaceutical institutions are now entering this interesting area of research. In this article, we describe a broadly applicable process for identifying degrader hits based on the serine/threonine kinase TANK-binding kinase 1 (TBK1) and have generalized the key structural elements associated with degradation activities. Compound **3i** is a potent hit (TBK1 $DC_{50}$ = 12 nM, $D_{max}$ = 96%) with excellent selectivity against a related kinase IKK$\varepsilon$, which was further used as a chemical tool to assess TBK1 as a target in mutant K-Ras cancer cells.

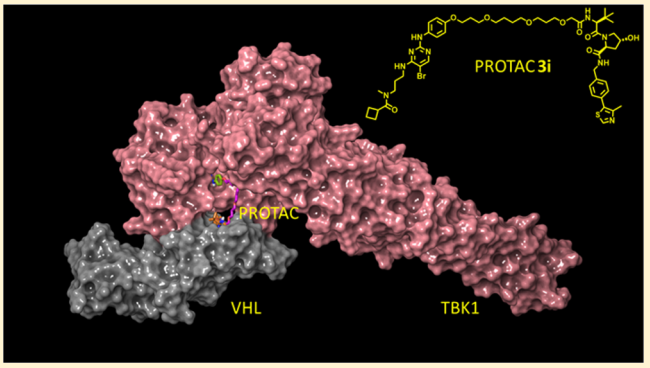


## INTRODUCTION

The most common therapeutic interventions available to the prescribing physician are inhibitor-based drugs such that the active pharmaceutical ingredient mediates the function of the aberrant protein via direct or allosteric *inhibition* of the mechanistic activity of the said protein. Although inhibition of protein activity is a clinically validated approach, there are significant constraints to its wider applicability. First, it usually carries the burden of requiring protracted target engagement for the mechanism and consequential function to be effectively abrogated. Many protein−small molecule interactions are associated with rapid off-rates, resulting in very low inhibitor occupancy of the protein active site and inadequate down-regulation of downstream signaling. Second, an inability to reach tolerated free-drug concentrations at or above the *in vitro* $IC_{90}$, because of high plasma protein binding, poor pharmacokinetics, or toxicity, can limit the effectiveness of inhibitor drugs. Finally, many proteins possess little or no mechanistic activity, yet execute their biological role by providing a scaffolding function, and as a result, these proteins are less susceptible to the inhibitor paradigm. For the reasons listed above, technologies that can reduce levels of a target protein in a manner that requires only transient interactions with the protein could provide significant therapeutic utility.

Proteolysis targeting chimeras (PROTACs),[1−9] are a class of bifunctional molecules that exist outside of the "rule of 5" (Ro5)[10] space that hijack the endogenous protein homeostasis machinery. As illustrated in Figure 1, PROTACs can recruit an E3 ubiquitin ligase to a target protein of interest (PoI), resulting in polyubiquitination of the PoI, which is subsequently degraded via the proteasome.[11] We have recently demonstrated the mechanism and the efficacy of our PROTAC technology by targeting a variety of proteins of interest for degradation, in both cultured cells and *in vivo*. These targets include the BET (bromodomain and extra terminal domain) family protein BRD4,[12] the serine/threonine kinase RIPK2,[13] and the estrogen related receptor $\alpha$ (ERR$\alpha$).[13] In this article, we describe for the first time the structural features governing the potency of PROTAC molecules, especially the effect of varying the effective distance between the two proteins by altering the length of the connecting linker and modulating the binding affinities to either the co-opted E3 ligase or target protein.

TANK-binding kinase 1 (TBK1) is a serine/threonine kinase and a noncanonical member of the IKK family implicated in

**Special Issue:** Inducing Protein Degradation as a Therapeutic Strategy

**Received:** May 4, 2017
**Published:** July 10, 2017





DOI: 10.1021/acs.jmedchem.7b00635
*J. Med. Chem.* 2018, 61, 583−598

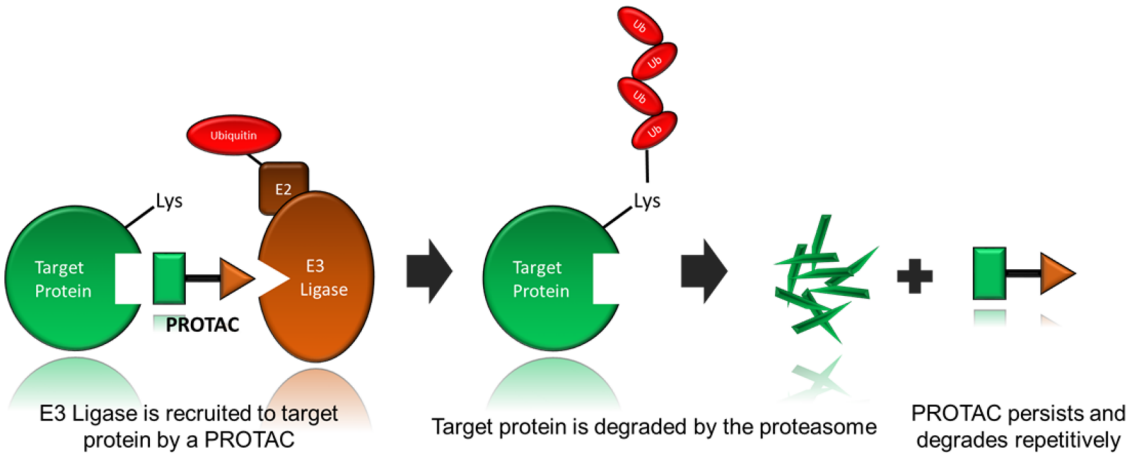


**Figure 1.** Protein degradation mediated by proteolysis targeting chimeras (PROTACs).

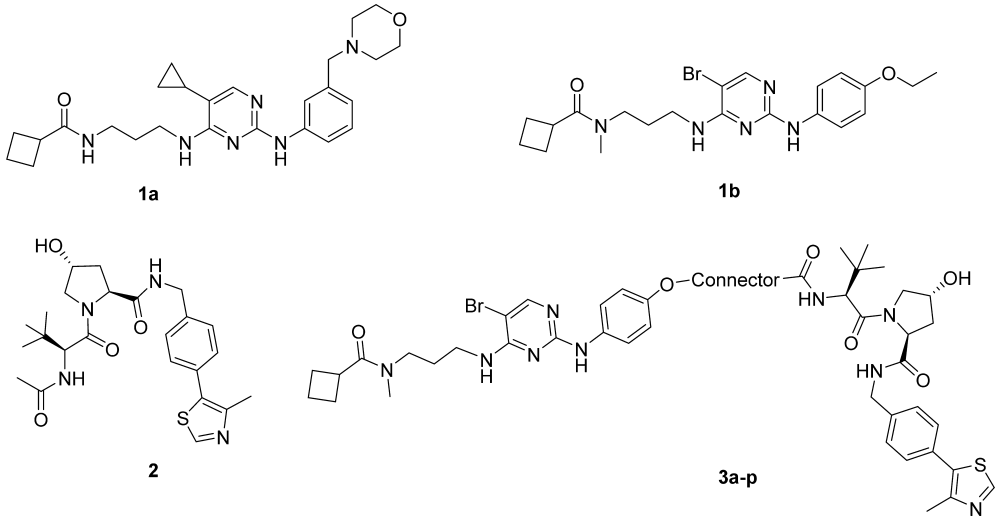


**Figure 2.** Structures of TBK1 ligands **1a** and **1b**, VHL ligand **2**, and TBK1 PROTACs **3a**–**p**.

diverse cellular functions, including innate immune response as well as tumorigenesis and development, that has attracted considerable attention with regard to the identification of agents that could diminish its activity.[14] Specifically, interest converged upon this protein in the wake of the purported critical role that TBK1 signaling plays in K-Ras mutant tumors as elucidated using RNAi.[15] However, subsequent reports challenged this hypothesis, and the synthetic lethality of TBK1 knockdown in this context was called into question.[16] In this study, we embarked on a campaign to assess whether TBK1 could be degraded using PROTAC technology to delineate the important structural features of active TBK1 PROTACs, with emphasis on each of the three components (target ligand, E3 ligase ligand, and linker), and finally, to determine whether a TBK1 PROTAC could replicate the K-Ras synthetic lethality reported with TBK1 RNAi.

## RESULTS AND DISCUSSION

PROTAC molecular architecture requires a protein targeting moiety (PTM) connected via a linker to an E3 ligase ligand. For the TBK1 PTM, we selected a classic kinase amino-pyrimidine chemotype for which a crystal structure of TBK1 bound to Compound **1a** was available (PDB code 4IM0).[17] Interrogation of the binding mode of compound **1a** in the TBK1 structure, in concert with the available SAR, indicated that an alternate egress point was available for linker attachment from the ligand out to solvent from the para-position of the pyrimidine-2-aminophenyl, and that a simple alkyl ether chemistry should be tolerated at this position. Additionally, it appeared that the NH of the secondary amide of compound **1a** was not providing any productive interactions with TBK1 and was likely adding a desolvation burden to the binding event suggesting an *N*-methyl derivative might be a beneficial modification. Combining these changes along with a bromo group in the 5-position of pyrimidine provided compound **1b** as a starting TBK1 PTM, which was confirmed to be a potent binder to TBK1 with a $K_d$ of 1.3 nM.

One of the E3 ligases with exciting therapeutic potential is the von Hippel-Lindau (VHL) tumor suppressor, which exists as part of an active E3 ubiquitin ligase complex.[18] Compound **2** is an example of a hydroxyproline derivative that binds to VHL to disrupt the VHL–HIF1$\alpha$ interaction[19] with an $IC_{50}$ of 0.8 $\mu$M in a fluorescence polarization (FP) assay. Structural information on a related analogue bound to the VHL-elongin/B-elongin C (VBC) complex (PDB code: 4W9H)[20] suggested the acetamide group in **2** would be tolerant to substitution and a good egress position from the protein for a linker. With both ligands **1b** and **2** in hand and the linker


DOI: 10.1021/acs.jmedchem.7b00635
J. Med. Chem. 2018, 61, 583–598

Table 1. Effect of Linker Length on the Degradation Activity of TBK1 PROTACs[a]

| Cmpd | Linker | # of linear non-H linker atoms | $DC_{50}$ (nM) | $D_{max}$ (%) | PSA (Å$^2$) |
|---|---|---|---|---|---|
| **1b** | NA | - | >1000 | ND | 79 |
| **2** | NA | - | >1000 | ND | 112 |
| **3a** | 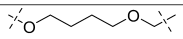 | 7 | >1000 | ND | 200 |
| **3b** | 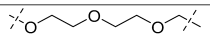 | 8 | >1000 | ND | 209 |
| **3c** | 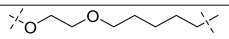 | 9 | >1000 | ND | 200 |
| **3d** | 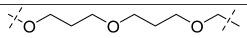 | 10 | >1000 | ND | 209 |
| **3e** | 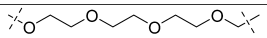 | 11 | >1000 | ND | 219 |
| **3f** | 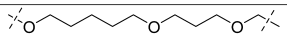 | 12 | 88 | 79 | 209 |
| **3g** | 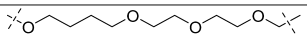 | 13 | 71 | 86 | 219 |
| **3h** | 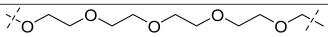 | 14 | 103 | 92 | 228 |
| **3i** | 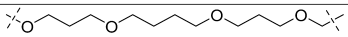 | 15 | 12 | 96 | 219 |
| **3j** | 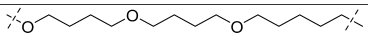 | 16 | 95 | 90 | 209 |
| **3k** | 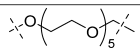 | 17 | 29 | 96 | 237 |
| **3l** | 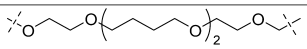 | 18 | 6 | 96 | 228 |
| **3m** | 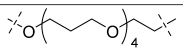 | 19 | 25 | 96 | 228 |
| **3n** | 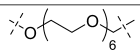 | 20 | 34 | 96 | 246 |
| **3o** | 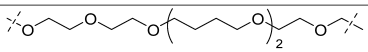 | 21 | 3 | 96 | 237 |
| **3p** | 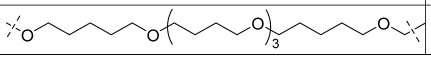 | 29 | 292 | 76 | 237 |

[a]NA: not applicable. ND: not determined. $DC_{50}$: concentration at which 50% degradation is observed. $D_{max}$: maximal degradation observed. Data represent the mean of ≥2 determinations. PSA calculations performed with ChemAxon software.

connection positions determined, we carried out a PROTAC design and synthesis campaign (**3a**–**p**, Figure 2).

We employed flexible and therefore accommodating alkyl ether chemistries to connect ligands **1b** and **2**, and not knowing *a priori* at what distance these ligands would have to be positioned in the PROTAC to effectively associate their respective proteins, we undertook a systematic survey of connector length. Table 1 lists the measured degradation potency ($DC_{50}$), maximum degradation observed ($D_{max}$), and the calculated two-dimensional polar surface area (PSA). From this initial library set, several PROTACs (**3f**–**3p**) were identified that degrade TBK1 with submicromolar potency. The gross SAR clearly indicates a dependence on a minimum linker length as PROTACs with linkers of <12 atoms demonstrated no appreciable degradation activity (**3a**–**3e**). Longer linkers appear generally well tolerated despite their higher PSA and presumed cell penetrance burden, such that even the 29-atom linker PROTAC **3p** still provided robust degradation albeit with reduced potency. These observations are consistent with the concept that the bifunctional PROTAC species mediates the association of the TBK1 and VHL proteins to form a ternary complex but that a minimum linker length is required to allow the proteins to come together without incurring steric conflicts. We hypothesize that the very flexible nature of the linker chemistry allows even the very long linkers to orient themselves so that the two proteins become associated for ubiquitin to transfer to TBK1. In addition, because each linker has a different composition and length, there will necessarily be differing contacts with the protein–protein interface which in turn will influence how strongly each derivative PROTAC can bind to and stabilize the ternary complex. This likely governs the efficiency of the key ubiquitin transfer and therefore contributes to the subtle degradation SAR seen across PROTACs **3f**–**3p**, along with differences in physicochemical properties. The formation of such a ternary complex mediated through bifunctional PROTACs was confirmed in the recently published crystal structure of MZ1, a BET PROTAC with a JQ1 carboxamide linked to VHL ligand **2**,[21] bound to both VHL and BRD4 proteins.[22]

To confirm the mechanistic dependence on VHL for TBK1 degradation, we prepared PROTAC **4** (Figure 3), an epimer of active PROTAC **3i**, which by nature of the reversed (*S*) stereochemistry at the proline 4-position has no appreciable



DOI: 10.1021/acs.jmedchem.7b00635
J. Med. Chem. 2018, 61, 583–598

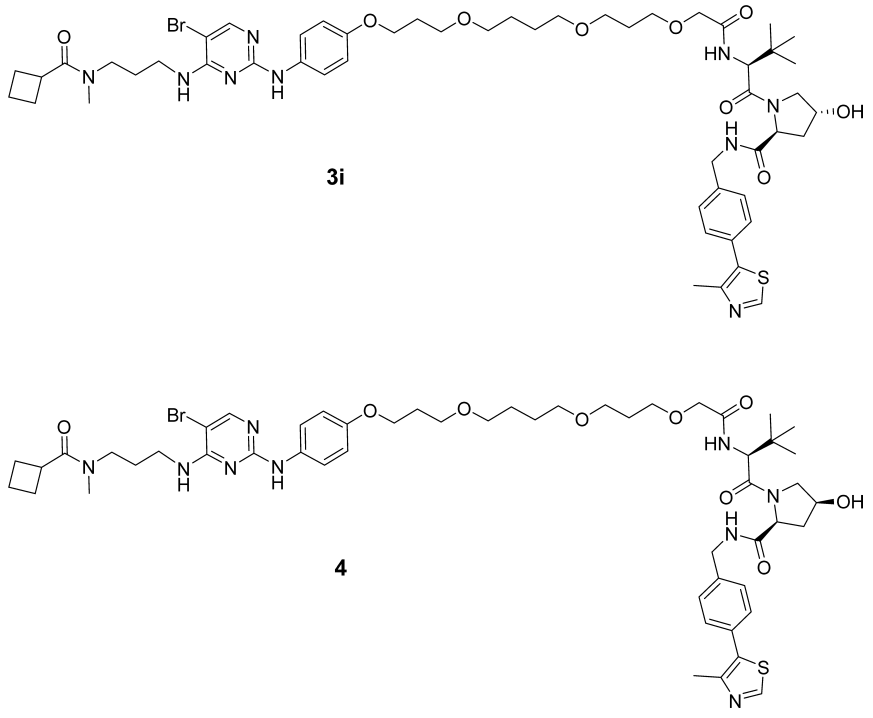


**Figure 3.** Structures of TBK1 degrader **3i** and its epimer **4**.

binding to VHL (FP $IC_{50}$ > 100 $\mu$M) but retained comparable TBK1 binding ($K_d$ = 5.9 nM for **4** versus 4.6 nM for **3i**).

PROTAC **4** showed no significant degradation of TBK1 (Figure 4), confirming VHL's role in the degradation of TBK1

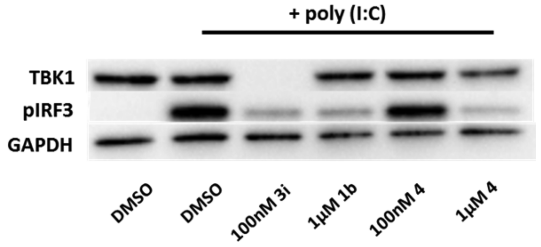


**Figure 4.** PROTAC **3i** but not its VHL-incompetent epimer **4** nor TBK1 inhibitor **1b** effects the degradation of TBK1. All three display competent intracellular TBK1/pIRF3 activity.

by PROTAC **3i**. The effect of **3i** and **4** on the TBK1 downstream marker pIRF3 was also assessed. Stimulation of Panc02.13 cells with Toll-like receptor 3 (TLR3) agonist polyinosine-polycytidylic acid [poly(I:C)] in the presence of both PROTAC agents as well as the parent TBK1 ligand **1b** confirmed competent intracellular TBK1 binding as indicated by the inhibition of pIRF3. The significantly more potent suppression of IRF3 phosphorylation by **3i** compared to **4** is indicative of the additional degradation activity afforded by **3i**, while **4** only exerted an antagonist effect.

The involvement of the proteasome in the VHL-mediated degradation of TBK1 by PROTAC **3i** was assessed by the addition of the proteasome inhibitor carfilzomib to the assay conditions. Pretreatment (30 min) with carfilzomib markedly reduced the extent of TBK1 degradation by PROTAC **3i** indicating that the 26S proteasome was indeed implicated in the degradation of TBK1 (Figure 5). Furthermore, addition of excess VHL ligand **2** to the assay to compete with PROTAC **3i** for VHL binding also abrogated TBK1's degradation.

With mechanistically specific tool degrader **3i** in hand, we next evaluated the impact of TBK1 binding affinity on degradation potency and efficiency. In order to minimize the impact of any cell permeation or conformational differences on observed degradation potency, we modified only the 5-position of the pyrimidine TBK1 ligand component and only used functionalities that did not substantially alter the polar surface

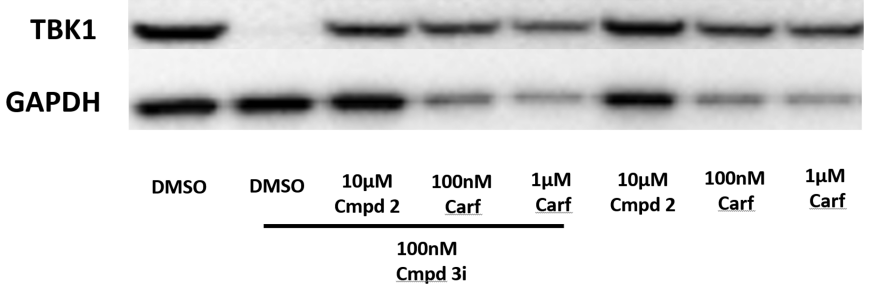


**Figure 5.** PROTAC **3i** mediated degradation of TBK1 is abrogated by pretreatment with either VHL ligand **2** or proteasome inhibitor carfilzomib (Carf).



DOI: 10.1021/acs.jmedchem.7b00635
J. Med. Chem. 2018, 61, 583−598

**Table 2. Effect of TBK1 Affinity on Degradation Activity**[a]

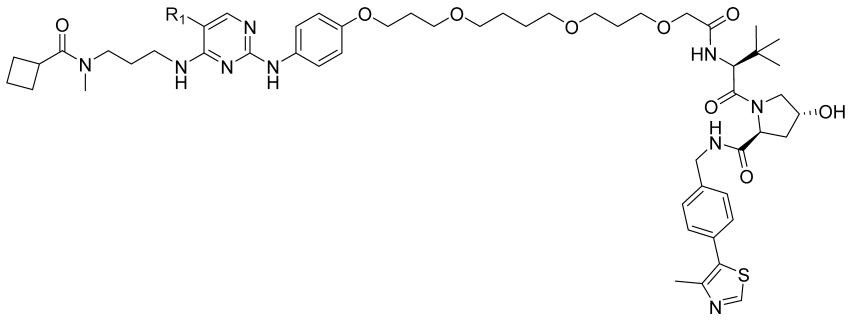

| compd | $R_1$ | TBK1 $K_d$ (nM) | $DC_{50}$ (nM) | $D_{max}$ (%) |
|---|---|---|---|---|
| **5a** | H | 725 | >1000 | ND |
| **5b** | F | 103.5 | 282 | 74 |
| **5c** | Cl | 10.4 | 10 | 96 |
| **5d** | I | 4 | 3 | 96 |
| **5e** | $CF_3$ | 13 | 29 | 96 |
| **5f** | Me | 270 | 92 | 89 |
| **5g** | Et | 275 | 121 | 77 |
| **5h** | cBu | 1035 | 544 | 70 |
| **5i** | vinyl | 130 | 48 | 96 |
| **5j** | cPr | 245 | 65 | 96 |
| **3i** | Br | 4.6 | 12 | 96 |

[a]ND: not determined. $DC_{50}$: concentration at which 50% degradation is observed. $D_{max}$: maximal degradation observed. Data represent the mean of ≥2 determinations.

**Table 3. Effect of VHL Affinity on Degradation Activity**

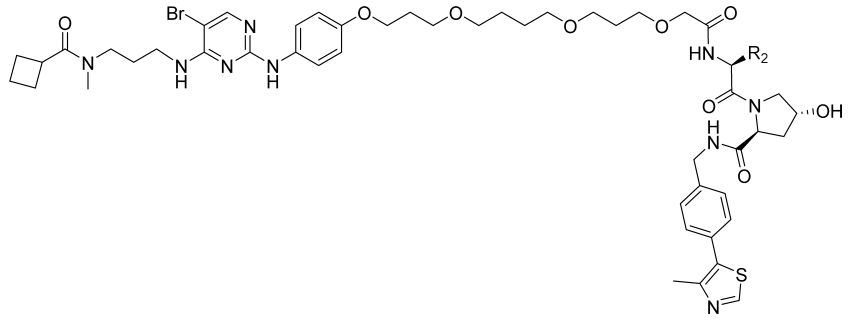

| cmpd | $R_2$ | PROTAC FP VHL $IC_{50}$ ($\mu$M) | $DC_{50}$ (nM) | $D_{max}$ (%) |
|---|---|---|---|---|
| **6a** | H | >100 | >1000 | 0 |
| **6b** | Me | 25.0 | >1000 | 34 |
| **6c** | Et | 9.9 | 864 | 71 |
| **6d** | $^{n}$Pr | 16.0 | 288 | 75 |
| **6e** | $^{i}$Pr | 5.5 | 44 | 88 |
| **3i** | $^{t}$Bu | 4.9 | 9 | 96 |

area of the set. Table 2 lists TBK1 binding affinities and the TBK1 degradation activity of these PROTACs.

Maximal efficacy (>90% degradation) was achieved with PROTACs that had TBK1 affinities ($K_d$) less than 245 nM, beyond which degradation begins to drop off, although remaining significant (70%) even in the case of compound **5h** that has a $K_d$ of 1 $\mu$M. The surprisingly high cellular degradation potency ($DC_{50}$ = 65 nM) seen with **5j**, in spite of its modest affinity for TBK1 ($K_d$ = 245 nM) and the relatively high $IC_{50}$ value of its VHL-binding component ligand ($IC_{50}$ = 800 nM), is likely due in part to the ability of the PROTAC to initiate multiple cycles of target protein degradation.[12] This is a mechanistic advantage of PROTAC technology over the traditional inhibitor paradigm that might prove to be of utility in the clinic where attaining a sufficiently high serum concentration of an inhibitor is a critical component for efficacy. Coupled with the longer-lasting effects of protein degradation on downstream signaling that we have already demonstrated elsewhere,[12,13] this result considerably strengthens the case for applying our technology to targets that prove intractable using conventional approaches and/or targets with low affinity ligands.

Next, we determined the effect of altering PROTAC VHL affinity, as measured in a fluorescence polarization (FP) assay, on PROTAC mediated degradation (Table 3). PROTACs **3i** and **6a**–**6e** differ in the side chain chemistry of the glycine component of the VHL ligand which, as for the TBK1 ligand, do not grossly change the molecular properties of the



DOI: 10.1021/acs.jmedchem.7b00635
J. Med. Chem. 2018, 61, 583–598

PROTACs (such as PSA) yet do alter their VHL affinity. Maximal efficacy was only seen with the parent PROTAC **3i** (R = *tert*-butyl; VHL ligand $IC_{50}$ = 4.9 $\mu$M), although robust degradation (>70%) was also seen with PROTACs **6c** and **6d** that displays up to 3-fold weaker VHL affinity. Interestingly, the fact that PROTAC **6b** did not show robust degradation activity despite displaying VHL affinity similar to that of **6d** is consistent with the operation of the more complex ternary system that that requires cooperative binding of the PROTAC to *both* proteins in play and suggests that the methyl group in **6b** is even more inferior at supporting this complex than the already suboptimal ethyl and *n*-propyl groups in **6c** and **6d**, respectively.

We next tested the ability of potent PROTAC **3i** to degrade the noncanonical IkB kinase IKK$\varepsilon$, a close homologue of TBK1, with which it shares 65% similarity. Since the TBK1 ligand used in the design of PROTAC **3i** exhibits poor selectivity for TBK1 over IKK$\varepsilon$ ($IC_{50}$ of 1.3 nM vs 8.7 nM), we expected substantial degradation of IKK$\varepsilon$ in our assays. To our surprise, PROTAC **3i** had no effect on the levels of IKK$\varepsilon$, at concentrations of more than 50-fold above its TBK1 $DC_{50}$ (Figure 6). We verified that PROTAC **3i** was capable of

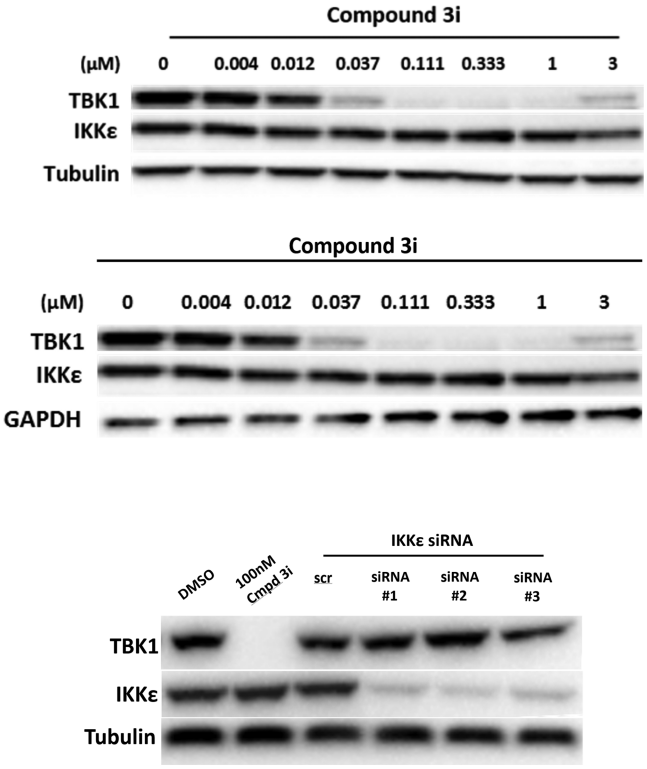


**Figure 6.** PROTAC **3i** selectively degrades TBK1 over IKK$\varepsilon$.

binding IKK$\varepsilon$ ($K_d$ = 70 nM) and that the observed band was IKK$\varepsilon$ through knock down with siRNA (Figure 6). As expected, scramble (scr) siRNA did not affect the IKK$\varepsilon$ levels, while three siRNAs completely knocked out the protein (Figure 6).

Since the reported $K_m$ values for ATP are not strikingly different for the two kinases,[23] we hypothesized that this introduction of degradation selectivity into a relatively unselective ligand likely results from a differential presentation of TBK1 and its surface lysines to VHL and its reactive E2-ubiquitin thioester component, as compared to IKK$\varepsilon$, and therefore a different pattern and/or efficiency of the transfer of ubiquitin to TBK1 (Figure 1). While such a difference in the formation and stability of the active trimer complexes could contribute to the selectivity, other potential explanations for this observation include an increased rate of deubiquitinylation in the case of IKK$\varepsilon$ or that IKK$\varepsilon$ ubiquitinylation by VHL results in an outcome other than protein degradation. Ubiquitination as a post-translational modification is known to serve a large variety of cellular functions,[24] and such an effect in the case of IKK$\varepsilon$ would be of considerable interest. A detailed investigation, however, is beyond the scope of the current article and will be left to a subsequent publication.

We next evaluated the effect of potent TBK1 degrader **3i** on cell lines harboring either wild-type or mutant K-Ras. Treatment of both K-Ras mutant cell lines (H23, A549, and H1792) and K-Rras wild type cell lines (H2110 and HCC827) with PROTAC **3i** for 72 h, while affecting near complete degradation of TBK1, caused no differential effect on the proliferation of these cells (Figures 7 and 8). This result is consistent with the literature reports that TBK1 was not synthetically lethal in K-Ras mutant versus wild type cells.[16]

**Chemistry.** The synthesis of TBK ligand **1b** is shown in Scheme 1. Starting from commercially available *N*-BOC protected amine **7**, amidation with cyclobutanecarboxylic acid, and subsequent removal of the BOC group generated amine **8**, which selectively displaced the 4-Cl of 5-bromo-2,4-dichloropyrimidine to afford compound **9**. Further $S_NAr$ reactions with 4-ethoxyaniline and 4-aminophenol under acidic conditions yielded the TBK1 ligand **1b** and key synthetic intermediate **10**. The VHL ligand **2** was prepared according to literature procedures,[14,15] and the preparation of VHL amino building blocks **18a−f** is shown in Scheme 2. Following Pd-catalyzed arylation of 4-bromobenzonitrile (**11**) and subsequent reduction with $LiAlH_4$, benzyl amine **13** was formed, which was coupled with *N*-BOC hydroxyproline (**14**) to give compound **15**. Upon deprotection of **15** with HCl/MeOH and subsequent amide formation with an $\alpha$-substituted *N*-BOC-glycine, intermediates **17a−f** were generated, which were BOC-deprotected to afford the corresponding VHL amino building blocks **18a−f**.

Scheme 3 illustrates two general approaches to synthesize PROTACs **3a−p**. In method A, the tosyl group of intermediate **20** was displaced by 4-nitrophenol, and the nitro group was reduced to provide amine **22**. This amine was reacted with 2-chloropyrimidine **9** to afford ester **23**, which was converted to its carboxylic acid and then coupled with VHL building block **18f** to afford the desired PROTACs. In method B, compound **23** was obtained in one step through the direct displacement of the tosyl group in **20** by the key intermediate **10**.

The syntheses of epimeric PROTAC **4** and PROTAC analogues **6a−e** are described in Scheme 4. Following the similar sequence as described in Scheme 2, the epimeric VHL amine building block **27** was prepared. The acid intermediate **24i** was coupled with different VHL amino building blocks **27** and **18a−e** to afford PROTACs **4** and **6a−e**, respectively.

For the exploration of the SAR of different TBK1 ligands, the acid derivative of linker **20i** was first coupled with the VHL amino building block **18f**, and the resulting tosylate **28** reacted with different TBK1 phenols **29a−j** to generate the corresponding PROTACs **5a−j** as displayed in Scheme 5. Debromination of **10** was achieved by hydrogenation over Pd−C to give phenol **29a**. For PROTACs with F, Cl, I, $CF_3$, Me, and Et at the 5-position of the pyrimidine ring, commercially


DOI: 10.1021/acs.jmedchem.7b00635
J. Med. Chem. 2018, 61, 583−598

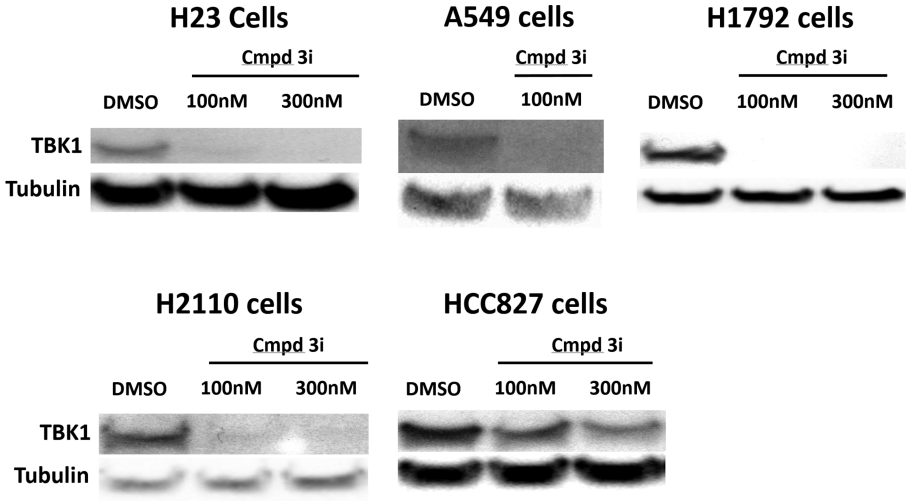


**Figure 7.** TBK1 degradation in K-Ras mutant and wild type cells (16 h of treatment).

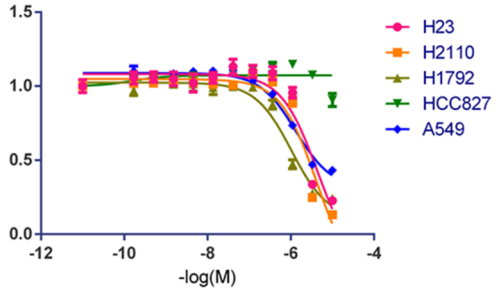


**Figure 8.** Relative proliferation of K-Ras mutant and wild type lung cancer cell lines in the presence of TBK1 degrader **3i** (72 h treatment; 10 $\mu$M top concentration).

available 2,4-dichloropyrimidines **30** were deployed, and a similar chemistry was followed to generate compounds **29b–g**. The introduction of cyclobutyl, vinyl, and cyclopropyl groups was achieved through Suzuki coupling reactions with **9**, followed by *SNAr* displacement by 4-aminophenol to give compounds **29h–j**.

## CONCLUSIONS

Herein, we have described a process for the rapid generation of potent, VHL, and proteasome-dependent PROTACs as degraders of TBK1, through a systematic survey of linker length and ligand affinities. We have also demonstrated that PROTACs can provide greater potency and selectivity than that anticipated based on the potency and selectivity of the component ligands. As targeted protein degradation with PROTACs and other molecules utilizing a similar mechanism has gained wider currency and validity in drug discovery, the study detailed herein could be used as a template for identifying degrader hits and leads, although for each protein targeted and ligase recruited, the affinity and linker length requirements will likely be different. Indeed, using this approach, we have successfully identified degrader leads across a variety of target protein classes, and our current efforts focused on optimizing those leads into orally active drug candidates. In subsequent publications, we will describe the breadth of this platform technology as it relates to other targets of interest and the achievement of oral activity.

## EXPERIMENTAL SECTION

**General Chemical Methods.** All reagents were obtained from commercial suppliers and used without further purification. Flash chromatography was performed using an ISCO CombiFlash RF 75 PSI with RediSep normal-phase silica gel cartridges. Preparative HPLC purification was performed on a Waters UV-directed purification system equipped with 2545 Binary Gradient Module. The mobile phases were water (0.1%TFA or 0.01% $NH_4HCO_3$) and acetonitrile with a flow rate of 30 mL/min. $^1$H NMR (300 or 400 MHz) and $^{13}$C NMR (100.6 MHz) spectra were recorded on Bruker spectrometers. Analytical LC-MS data were collected on a Shimadzu LCMS-2020 with mobile phases as acetonitrile and water containing 0.05% TFA.

**Scheme 1. Syntheses of TBK1 Ligand 1b and Key Intermediate 10**[a]

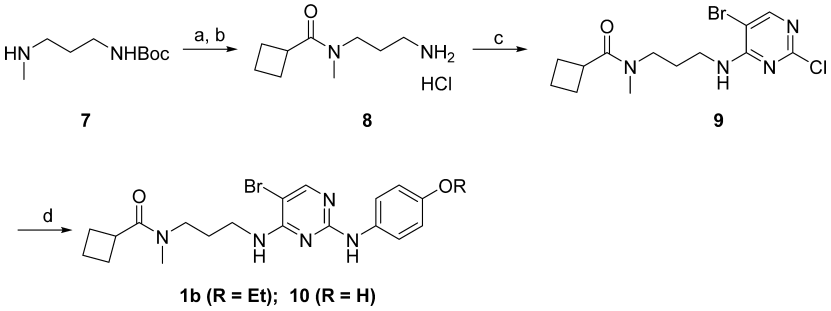


[a]Reagents and conditions: (a) cyclobutanecarboxylic acid, HATU, DIPEA, DMF, rt, overnight; (b) HCl, MeOH, rt, 1 h; (c) 5-bromo-2,4-dichloropyrimidine, DIPEA, MeCN, rt, 3 h; (d) substituted anilines, dioxane, TsOH, 90 °C, overnight.



DOI: 10.1021/acs.jmedchem.7b00635
J. Med. Chem. 2018, 61, 583–598

**Scheme 2. Syntheses of VHL Amino Building Blocks**[a]

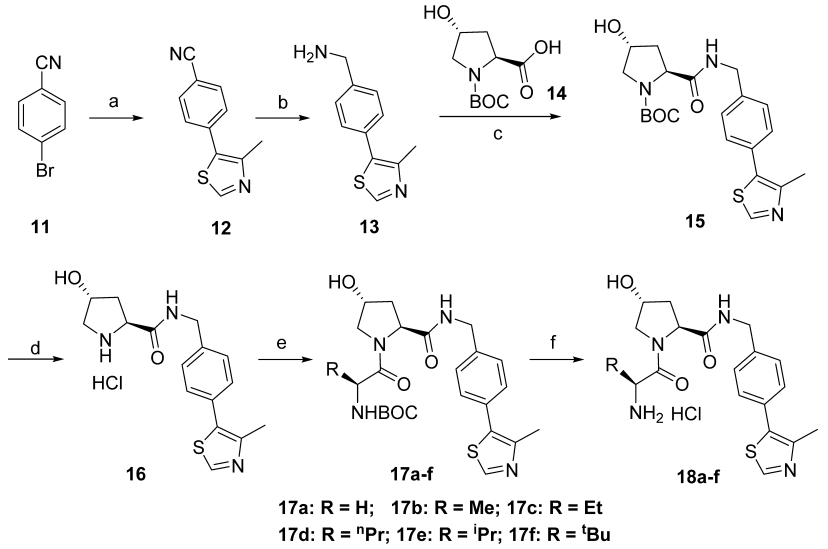


[a]Reagents and conditions: (a) 4-methylthiazole, $Pd(OAc)_2$, DMA, 150 °C, 5 h; (b) $LiAlH_4$, THF, reflux, 5 h; (c) **14**, HATU, DIPEA, DMF, rt, 2 h; (d) HCl, MeOH, 2 h; (e) *N*-BOC amino acids, HATU, DIPEA, DMF, rt, 3 h; (f) HCl, MeOH, rt, 3 h.

**Scheme 3. Syntheses of TBK1 PROTACs 3a−3p**[a]

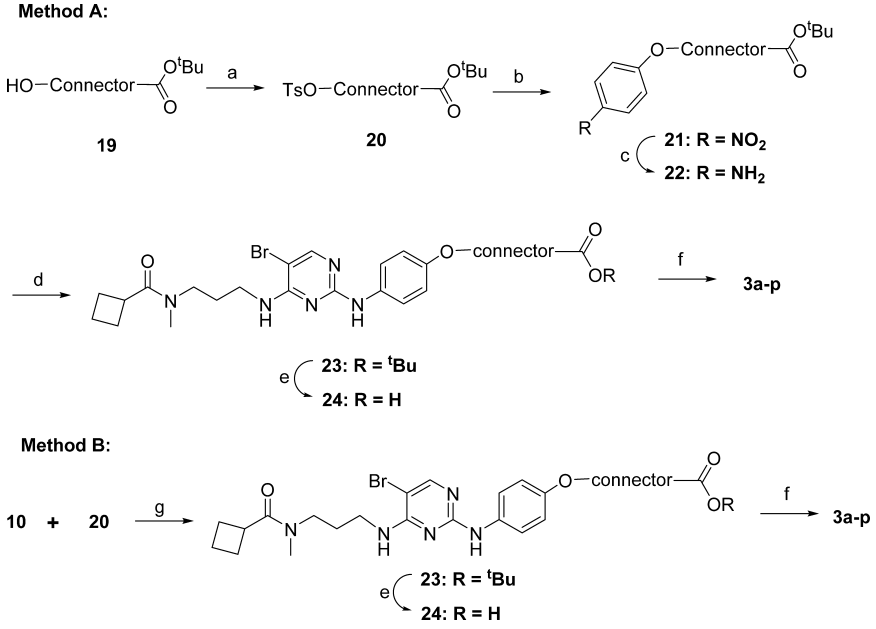


[a]Reagents and conditions: (a) *p*-TsCl, $NEt_3$, cat. DMAP, DCM, rt, overnight; (b) 4-nitrophenol, $K_2CO_3$, DMF, 70 °C, overnight; (c) Pd/C, $H_2$, EtOH, rt, overnight; (d) **9**, *p*-TsOH, dioxane, 100 °C, overnight; (e) 4 N HCl/dioxane, rt, overnight; (f) **18f**, HATU, DIPEA, DMF, rt, 1 h; (g) $Cs_2CO_3$, 80 °C, overnight.

The purities of all final compounds were over 95% as determined by LC-MS analysis monitored at 214 and 254 nM.

*N-[3-({5-Bromo-2-[(4-ethoxyphenyl)amino]pyrimidin-4-yl}-amino)propyl]-N-methylcyclobutanecarboxamide (**1b**).* A solution containing **9** (50 mg, 0.14 mmol), 4-ethoxyaniline (47 mg, 0.35 mmol), 4 N HCl in 1,4-dioxane (0.10 mL), and *n*-butanol (1 mL) was heated in a microwave oven at 120 °C for 40 min. The reaction mixture was concentrated, and the residue was purified using a Teledyne Combiflash (0 to 3% 7 N $NH_3$/MeOH in DCM) to afford compound **1** as an off white solid (64 mg, 99% yield). $^1H$ NMR (400 MHz, $CD_3OD$) $\delta$ 7.83 (2*s*, 1H), 7.42 (d, $J$ = 9.0 Hz, 2H), 6.78−6.87 (m, 2H), 3.97 (2*q*, $J$ = 7.0 Hz, 2H), 3.31−3.47 (m, 4H), 3.17−3.26 (m, 1H), 2.84 (2*s*, 3H), 2.10−2.24 (m, 3H), 1.88−2.03 (m, 2H), 1.69−1.87 (m, 3H), 1.34 (t, $J$ = 7.0 Hz, 3H). LC-MS ($ES^+$): $m/z$ 461.9 and 463.9 [M + $H^+$].

**General Procedure for Preparing PROTACs Using Method A As Described in Scheme 3.** *(2S,4R)-1-[(2S)-2-[2-(4-{4-[(5-Bromo-4-{[3-(1-cyclobutyl-N-methylformamido)propyl]amino}pyrimidin-2-yl)amino]phenoxy}butoxy)acetamido]-3,3-dimethylbutanoyl]-4-hydroxy-N-{[4-(4-methyl-1,3-thiazol-5-yl)phenyl]methyl}pyrrolidine-2-carboxamide (**3a**).* A mixture of **21a** (600 mg, 1.8 mmol) and palladium on carbon (10%, 60 mg) in ethanol (20 mL) was stirred under hydrogen atmosphere at rt overnight. The mixture was filtered and washed with ethanol. The filtrate was concentrated under reduced pressure to afford *tert*-butyl 2-(4-(4-aminophenoxy)butoxy)acetate (**22a**) as a colorless oil (550 mg, 90% yield). This oily material (82 mg, 0.28 mmol) was mixed with compound **9** (100 mg, 0.28 mmol) and


DOI: 10.1021/acs.jmedchem.7b00635
J. Med. Chem. 2018, 61, 583−598

**Scheme 4. Syntheses of TBK1 PROTACs 4 and 6a−e**[a]

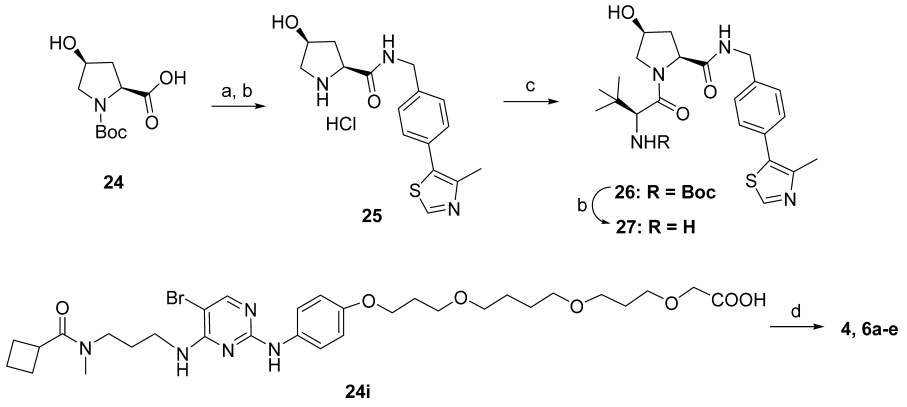


[a]Reagents and conditions: (a) **13**, HATU, DIPEA, DMF, rt, overnight; (b) HCl, MeOH, rt, 2 h; (c) *N*-Boc L-*tert*-leucine, HATU, DIPEA, DMF, rt, overnight; (d) **27** or **18a−e**, HATU, DIPEA, DMF, rt, 2 h.

**Scheme 5. Syntheses of TBK1 PROTACs 5a−j**[a]

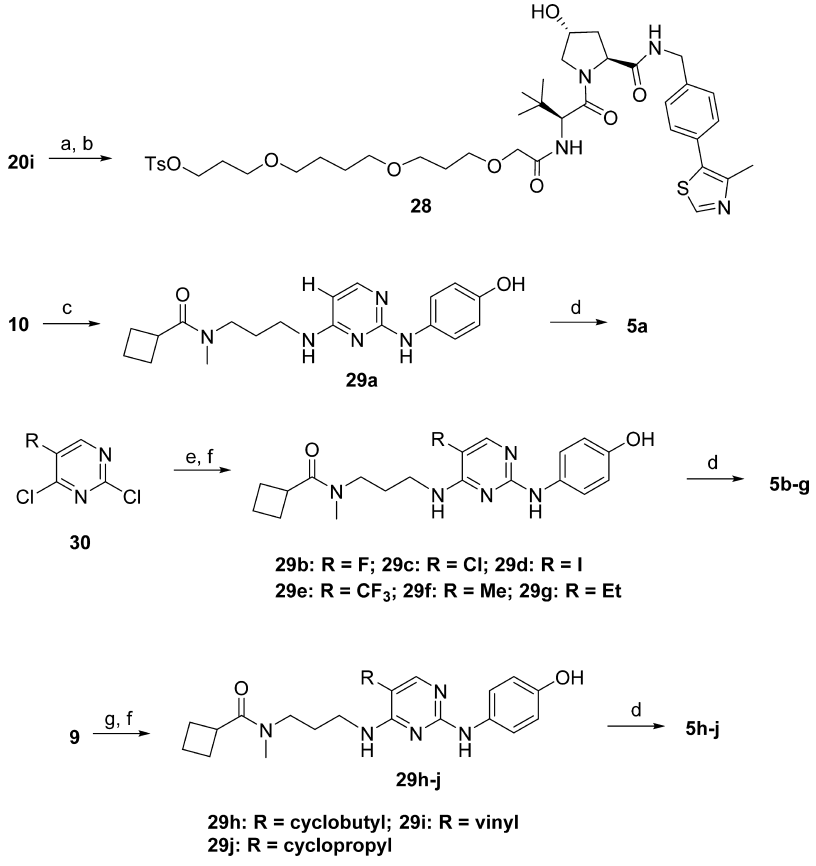


[a]Reagents and conditions: (a) TFA, DCM, rt, 3 h; (b) **18f**, HATU, DIPEA, DMF, rt, 2 h; (c) Pd/C, $H_2$, MeOH, rt, 0.5 h; (d) **28**, $Cs_2CO_3$, 80 °C, 5 h; (e) **8**, DIPEA, MeCN, rt, overnight; (f) 4-aminophenol, *p*-TsOH, dioxane, 90 °C, overnight; (g) $RB(OH)_2$, $PdCl_2(dppf)$, $Na_2CO_3$, toluene/water, 100 °C, 3 h.

toluene sulfonic acid monohydrate (19 mg, 0.1 mmol) in dioxane (3 mL), and the mixture was stirred at 100 °C for 16 h. The reaction mixture was first cooled to rt and then partitioned between ethyl acetate and aqueous $NaHCO_3$ solution. The organic phase was washed with water, brine, dried over anhydrous sodium sulfate, and concentrated. The residue was purified by silica gel column chromatography using 2%−5% MeOH in dichloromethane as eluent to afford *tert*-butyl 2-(4-(4-(5-bromo-4-(3-(*N*-methylcyclobutanecarboxamido)propylamino)pyrimidin-2-ylamino)-phenoxy)butoxy)acetate (**23a**) as a yellow oil (60 mg, 35% yield). LC-MS (ES$^+$): *m*/*z* 620.2 and 622.2 [M + H$^+$]. This oil (60 mg, 0.1 mmol) in 4 M HCl/dioxane (2 mL) was stirred at rt for 1 h. The reaction mixture was concentrated under reduced pressure to provide 2-(4-(4-(5-bromo-4-(3-(*N*-methylcyclobutanecarboxamido)-propylamino)pyrimidin-2-ylamino)phenoxy)butoxy)acetic acid (**24a**) as a yellow oil (55 mg, 95% yield). Carboxylic acid **24a** (55 mg, 0.1 mmol) was mixed with **18f** (45 mg, 0.1 mmol) and DIPEA (46 mg, 0.36 mmol) in dry DMF (3 mL). To this solution was added HATU (74 mg, 0.2 mmol) at 0 °C. The resulting mixture was stirred at rt for 0.5 h. The mixture was partitioned between ethyl acetate and water.



DOI: 10.1021/acs.jmedchem.7b00635
*J. Med. Chem.* 2018, 61, 583−598

The organic phase was washed with water and brine and dried over anhydrous sodium sulfate, filtered, and concentrated. The residue was purified by preparative TLC to afford the desired product **3a** as a white solid (19 mg, 20% yield). $^1$H NMR (400 MHz, $CD_3OD$): $\delta$ 1.03, 1.05 (two singlets, 9H), 1.79−2.26 (m, 15H), 2.48 (s, 3H), 2.85−2.91 (2s, 3H), 3.27 (t, $J$ = 7.2 Hz, 1H), 3.42−3.50 (m, 3H), 3.65 (t, $J$ = 6.0 Hz, 2H), 3.79−4.07 (m, 6H), 4.34−4.39 (m, 1H), 4.52−4.62 (m, 3H), 4.72 (t, $J$ = 6.8 Hz, 1H), 6.85−6.91 (m, 2H), 7.41−7.49 (m, 6H), 7.59 (d, $J$ = 9.2 Hz, 1H, exchanged H), 7.87 (2s, 1H), 8.87 (s, 1H). LC-MS (ES$^+$): $m/z$ 976.2/978.2 [M + H$^+$].

**General Procedure for Preparing PROTACs Using Method B As Described in Scheme 3.** *(2S,4R)-1-[(2S)-2-(1-{4-[(5-Bromo-4-{[3-(1-cyclobutyl-N-methylformamido)propyl]amino}pyrimidin-2-yl)amino]phenyl}-1,5,10,14-tetraoxahexadecan-16-amido)-3,3-dimethylbutanoyl]-4-hydroxy-N-{[4-(4-methyl-1,3-thiazol-5-yl)-phenyl]methyl}pyrrolidine-2-carboxamide (**3i**).* A mixture of *tert*-butyl 2-[3-[4-(3-hydroxypropoxy)butoxy]propoxy]acetate (**19i**, 230 mg, 0.66 mmol), toluene sulfonyl chloride (189 mg, 0.99 mmol), triethylamine (134 mg, 1.32 mmol), and DMAP (16 mg) in dichloromethane (5 mL) was stirred at rt for 4 h. The reaction mixture was diluted with dichloromethane (100 mL) and washed with water and brine. The organic layer was dried over sodium sulfate, filtered, and concentrated. The residue was purified by silica gel column chromatography using 30% EtOAc in hexanes as eluent to afford *tert*-butyl 2-[3-(4-{3-[(4-methylbenzenesulfonyl)oxy]propoxy}-butoxy)propoxy]acetate (**20i**) as a colorless oil (250 mg, 73% yield). LC-MS (ES$^+$): $m/z$ 492.2 [M + NH$_4^+$]. This material (105 mg, 0.22 mmol) was mixed with **10** (80 mg, 0.18 mmol), cesium carbonate (120 mg, 0.37 mmol) in *N*,*N*-dimethylformamide (5 mL), and the mixture was stirred at 80 °C overnight. The mixture was diluted with water (20 mL) and extracted with ethyl acetate (50 mL × 2). The combined organic layers were washed with brine (50 mL × 2) and dried over anhydrous sodium sulfate. The residue was purified by silica gel column chromatography using ethyl acetate/petroleum ether (7/3) as eluent to afford *tert*-butyl 1-{4-[(5-bromo-4-{[3-(1-cyclobutyl-*N*-methylformamido)propyl]amino}pyrimidin-2-yl)amino]phenyl}-1,5,10,14-tetraoxahexadecan-16-oate (**23i**) as a black oil (100 mg, 74% yield). LC-MS (ES$^+$): $m/z$ 736.4/738.4 [M + H$^+$]. The *tert*-butyl ester **23i** (100 mg, 0.14 mmol) in dichloromethane (5 mL) and trifluoroacetic acid (3 mL) was stirred at rt for 2 h. The reaction mixture was concentrated under reduced pressure to provide the corresponding carboxylic acid **24i** as a black oil (92 mg, 100% yield). LC-MS (ES$^+$): $m/z$ 680.3/682.3 [M + H$^+$]. This carboxylic acid **24i** (100 mg, 0.147 mmol) was mixed with **18f** (68 mg, 0.147 mmol) and DIPEA (77 mg, 0.6 mmol) in dry DMF (3 mL), and HATU (114 mg, 0.3 mmol) was added at 0 °C. The resulting mixture was stirred at rt for 0.5 h. The mixture was partitioned between ethyl acetate and water. The organic phase was washed with water and brine and dried over anhydrous sodium sulfate, filtered, and concentrated. The residue was purified by preparative TLC to afford **3i** as a white solid (22.5 mg, 15% yield). $^1$H NMR (400 MHz, $CD_3OD$): $\delta$ 1.05 (s, 9H), 1.60−1.64 (m, 4H), 1.80−2.26 (m, 15H), 2.48 (s, 3H), 2.86−2.91 (2s, 3H), 3.26−3.28 (m, 1H), 3.40−3.54 (m, 9H), 3.59−3.64 (m, 4H), 3.83−3.88 (m, 2H), 3.97−4.06 (m, 4H), 4.34−4.38 (m, 1H), 4.52−4.61 (m, 3H), 4.71−4.72 (m, 1H), 6.87−6.90 (m, 2H), 7.41−7.49 (m, 6H), 7.87−7.90 (2s, 1H), 8.88 (s, 1H). LC-MS (ES$^+$): $m/z$ 1092.5 and 1094.5 [M + H$^+$].

**PROTACs Prepared According to Method A As Described in Scheme 3: 3b, 3d, 3e, 3g, 3h, 3k, and 3n.** *(2S,4R)-1-[(2S)-2-{2-[2-(2-{4-[(5-Bromo-4-{[3-(1-cyclobutyl-N-methylformamido)propyl]-amino}pyrimidin-2-yl)amino]phenoxy}ethoxy)ethoxy]acetamido}-3,3-dimethylbutanoyl]-4-hydroxy-N-{[4-(4-methyl-1,3-thiazol-5-yl)-phenyl]methyl}pyrrolidine-2-carboxamide (**3b**).* $^1$H NMR (400 MHz, $CDCl_3$): $\delta$ 0.95 (s, 9H), 1.74−1.77 (m, 2H), 1.85−1.90 (m, 2H), 1.94−2.01 (m, 1H), 2.14−2.20 (m, 3H), 2.33−2.37 (m, 2H), 2.45−2.54 (m, 4H), 2.89 (s, 3H), 3.25−3.32 (m, 1H), 3.40−3.49 (m, 4H), 3.60−3.73 (m, 5H), 3.84 (d, $J$ = 4.8 Hz, 2H), 3.93−4.02 (m, 2H), 4.10−4.15 (m, 3H), 4.29−4.34 (m, 1H), 4.46−4.58 (m, 3H), 4.74 (t, $J$ = 8.0 Hz, 1H), 6.57 (br, 1H), 6.86−6.88 (m, 2H), 7.25−7.26 (m, 1H), 7.34−7.36 (m, 4H), 7.43−7.45 (m, 2H), 7.56−7.59 (m, 1H), 7.87−7.93 (2s, 1H), 8.78(s, 1H). LC-MS (ES+): $m/z$ 992.3 and 994.3 [M + H$^+$].

*(2S,4R)-1-[(2S)-2-{2-[3-(3-{4-[(5-Bromo-4-{[3-(1-cyclobutyl-N-methylformamido)propyl]amino}pyrimidin-2-yl)amino]phenoxy}-propoxy)propoxy]acetamido}-3,3-dimethylbutanoyl]-4-hydroxy-N-{[4-(4-methyl-1,3-thiazol-5-yl)phenyl]methyl}pyrrolidine-2-carboxamide (**3d**).* $^1$H NMR (400 MHz, $CD_3OD$): $\delta$ 1.05 (t, $J$ = 7.2 Hz, 9H), 1.38−1.41 (m, 4H), 1.83−1.92 (m, 3H), 1.98−2.12 (m, 4H), 2.18−2.29 (m, 4H), 2.48 (2s, 3H), 2.88 (multiple s, 3H), 3.24 (m, 1H), 3.38−3.65 (m, 9H), 3.75−4.06 (m, 6H), 4.35 (d, $J$ = 15.6 Hz, 1H), 4.49−4.62 (m, 3H), 4.71 (t, $J$ = 6.8 Hz, 1H), 6.85−6.90 (m, 2H), 7.40−7.56 (m, 6H), 7.87 (2s, 1H), 8.87−8.90 (s and m, 1H). LC-MS (ES$^+$): $m/z$ 1020.2 and 1022.2 [M + H$^+$].

*(2S,4R)-1-[(2S)-2-(1-{4-[(5-Bromo-4-{[3-(1-cyclobutyl-N-methylformamido)propyl]amino}pyrimidin-2-yl)amino]phenyl}-1,4,7,10-tetraoxadodecan-12-amido)-3,3-dimethylbutanoyl]-4-hydroxy-N-{[4-(4-methyl-1,3-thiazol-5-yl)phenyl]methyl}pyrrolidine-2-carboxamide (**3e**).* $^1$H NMR (400 MHz, $CD_3OD$): $\delta$ 1.06 (s, 9H), 1.80−2.23 (m, 11H), 2.48 (s, 3H), 2.86−2.91 (2s, 3H), 3.26−3.30 (m, 1H), 3.40−3.45 (m, 3H), 3.71−3.73 (m, 8H), 3.81−3.88 (m, 4H), 4.04−4.11 (m, 4H), 4.34−4.38 (m, 1H), 4.52−4.59 (m, 3H), 4.70−4.73 (m, 1H), 6.88−6.91 (m, 2H), 7.40−7.49 (m, 6H), 7.66−7.69 (2 br s, 1H, exchanged H), 7.86−7.89 (2s, 1H), 8.87 (s, 1H). LC-MS (ES$^+$): $m/z$ 1036.1/1038.1 [M + H$^+$].

*(2S,4R)-1-[(2S)-2-(1-{4-[(5-Bromo-4-{[3-(1-cyclobutyl-N-methylformamido)propyl]amino}pyrimidin-2-yl)amino]phenyl}-1,6,9,12-tetraoxatetradecan-14-amido)-3,3-dimethylbutanoyl]-4-hydroxy-N-{[4-(4-methyl-1,3-thiazol-5-yl)phenyl]methyl}-pyrrolidine-2-carboxamide (**3g**).* $^1$H NMR (400 MHz,$CD_3OD$): $\delta$ 0.94 (s, 9H), 1.62−1.72 (m, 7H), 1.75−1.96 (m, 4H), 2.08−2.12 (m, 4H), 2.36 (s, 3H), 2.74−2.79 (2s, 3H), 3.14−3.16 (m, 1H), 3.31−3.42 (m, 5H), 3.50−3.60 (m, 8H), 3.68−3.79 (m, 2H), 3.84−3.94 (m, 4H), 4.22−4.24 (m, 1H), 4.40−4.47 (m, 3H), 4.58−4.60 (m, 1H), 6.73−6.79 (m, 2H), 7.29−7.36 (m, 6H), 7.74−7.77 (2s, 1H), 8.76 (s, 1H). LC-MS (ES$^+$): $m/z$ 1064.2 and 1066.2 [M + H$^+$].

*(2S,4R)-1-[(2S)-2-(1-{4-[(5-Bromo-4-{[3-(1-cyclobutyl-N-methylformamido)propyl]amino}pyrimidin-2-yl)amino]phenyl}-1,4,7,10,13-pentaoxapentadecan-15-amido)-3,3-dimethylbutanoyl]-4-hydroxy-N-{[4-(4-methyl-1,3-thiazol-5-yl)phenyl]methyl}-pyrrolidine-2-carboxamide (**3h**).* $^1$H NMR (400 MHz, $CD_3OD$): $\delta$ 1.06 (s, 9H), 1.81−1.85 (m, 3H), 2.01−2.26 (m, 8H), 2.50 (s, 3H), 2.85−2.93 (2 br s, 3H), 3.42−3.49 (m, 4H), 3.67−3.87 (m, 15H), 4.01−4.05 (m, 3H), 4.14−4.17 (m, 2H), 4.35−4.39 (m, 1H), 4.52−4.58 (m, 3H), 4.70−4.73 (m, 1H), 7.03−7.07 (m, 2H), 7.35−7.49 (m, 6H), 7.66−7.68 (2s, 1H, exchanged H), 7.93−7.98 (2 br s, 1H), 8.94 (s, 1H). LC-MS (ES$^+$): $m/z$ 1080.2 and 1082.2 [M + H$^+$].

*(2S,4R)-1-[(2S)-2-(1-{4-[(5-Bromo-4-{[3-(1-cyclobutyl-N-methylformamido)propyl]amino}pyrimidin-2-yl)amino]phenyl}-1,4,7,10,13,16-hexaoxaoctadecan-18-amido)-3,3-dimethylbutanoyl]-4-hydroxy-N-{[4-(4-methyl-1,3-thiazol-5-yl)phenyl]methyl}-pyrrolidine-2-carboxamide (**3k**).* $^1$H NMR (400 MHz, $CD_3OD$): $\delta$ 1.06 (s, 9H), 1.80−2.23 (m, 11H), 2.48 (s, 3H), 2.86−2.91 (2s, 3H), 3.26−3.28 (m, 1H), 3.42−3.49 (m, 3H), 3.60−3.70 (m, 17H), 3.79−3.84 (m, 3H), 3.88−3.90 (m, 1H), 4.04−4.12 (m, 4H), 4.34−4.38 (m, 1H), 4.51−4.54 (m, 1H), 4.58−4.62 (m, 1H), 4.71−4.72 (m, 1H), 6.88−6.92 (m, 2H), 7.41−7.50 (m, 6H), 7.87−7.90 (2s, 1H), 8.88 (s, 1H). LC-MS (ES$^+$): $m/z$ 1124.4 and 1126.4 [M + H$^+$].

*(2S,4R)-1-[(2S)-2-(1-{4-[(5-Bromo-4-{[3-(1-cyclobutyl-N-methylformamido)propyl]amino}pyrimidin-2-yl)amino]phenyl}-1,4,7,10,13,16,19-heptaoxahenicosan-21-amido)-3,3-dimethylbutanoyl]-4-hydroxy-N-{[4-(4-methyl-1,3-thiazol-5-yl)phenyl]methyl}-pyrrolidine-2-carboxamide (**3n**).* $^1$H NMR (400 MHz, $CD_3OD$): $\delta$ 1.06 (s, 9H), 1.81−1.86 (m, 4H), 2.01−2.04 (m, 3H), 2.18−2.26 (m, 4H), 2.48 (s, 3H), 2.86−2.91 (2s, 3H), 3.43−3.46 (m, 4H), 3.60−3.69 (m, 20H), 3.83−3.85 (m, 4H), 4.04−4.11 (m, 4H), 4.34−4.38 (m, 1H), 4.52−4.59 (m, 3H), 4.71−4.72 (m, 1H), 6.90−6.93 (m, 2H), 7.41−7.51 (m, 6H), 7.87−7.90 (2s, 1H), 8.89 (s, 1H). LC-MS (ES$^+$): $m/z$ 1168.4 and 1170.4 [M + H$^+$].

**PROTACs Prepared According to Method B As Described in Scheme 3: 3c, 3f, 3j, 3l, 3m, 3o, and 3p.** *(2S,4R)-1-[(2S)-2-[6-(2-{4-[(5-Bromo-4-{[3-(1-cyclobutyl-N-methylformamido)propyl]amino}-pyrimidin-2-yl)amino]phenoxy}ethoxy)hexanamido]-3,3-dimethyl-butanoyl]-4-hydroxy-N-{[4-(4-methyl-1,3-thiazol-5-yl)phenyl]-*


DOI: 10.1021/acs.jmedchem.7b00635
J. Med. Chem. 2018, 61, 583−598

*methyl}pyrrolidine-2-carboxamide (**3c**).* $^1$H NMR (400 MHz, $CDCl_3$): $\delta$ 0.95 (s, 9H), 1.74−1.77 (m, 2H), 1.85−1.90 (m, 2H), 1.94−2.01 (m, 1H), 2.14−2.20 (m, 3H), 2.33−2.37 (m, 2H), 2.45−2.54 (m, 4H), 2.89 (s, 3H), 3.25−3.32 (m, 1H), 3.40−3.49 (m, 4H), 3.60−3.73 (m, 5H), 3.84 (d, $J$ = 4.8 Hz, 2H), 3.93−4.02 (m, 2H), 4.10−4.15 (m, 3H), 4.29−4.34 (m, 1H), 4.46−4.58 (m, 3H), 4.74 (t, $J$ = 8.0 Hz, 1H), 6.57 (br, 1H), 6.86−6.88 (m, 2H), 7.25−7.26 (m, 1H), 7.34−7.36 (m, 4H), 7.43−7.45 (m, 2H), 7.56−7.59 (m, 1H), 7.87−7.93 (2s, 1H), 8.78 (s, 1H). LC-MS (ES$^+$): $m/z$ 1004.4 and 1006.4 [M + H$^+$].

*(2S,4R)-1-[(2S)-2-(2-{3-[(5-{4-[(5-Bromo-4-{[3-(1-cyclobutyl-N-methylformamido)propyl]amino}pyrimidin-2-yl)amino]phenoxy}-pentyl)oxy]propoxy}acetamido)-3,3-dimethylbutanoyl]-4-hydroxy-N-{[4-(4-methyl-1,3-thiazol-5-yl)phenyl]methyl}pyrrolidine-2-carboxamide (**3f**).* $^1$H NMR (400 MHz, DMSO-$d_6$): $\delta$ 8.98 (m, 2H), 8.60 (m, 1H), 7.97 (d, $J$ = 7.6 Hz, 1H), 7.57 (d, $J$ = 7.6 Hz, 2H), 7.35−7.40 (m, 5H), 7.05−6.95 (m, 1H), 6.85−6.82 (m, 2H), 5.15 (s, 1H), 4.58−4.21 (m, 5H), 3.92−3.88 (m, 4H), 3.69−3.41 (m, 6H), 3.37 (m, 5H), 3.19 (m, 1H), 2.82−2.75 (2s, 3H), 2.45 (s, 3H), 2.20−1.65 (m, 15H), 1.58−1.50 (m, 2H), 1.47−1.40 (m, 2H), 0.94 (s, 9H). LC-MS (ES$^+$): $m/z$ 1048.2 and 1050.2 [MH$^+$].

*(2S,4R)-1-[(2S)-2-{6-[4-(4-{4-[(5-Bromo-4-{[3-(1-cyclobutyl-N-methylformamido)propyl]amino}pyrimidin-2-yl)amino]phenoxy}-butoxy)butoxy]hexanamido}-3,3-dimethylbutanoyl]-4-hydroxy-N-{[4-(4-methyl-1,3-thiazol-5-yl)phenyl]methyl}pyrrolidine-2-carboxamide (**3j**).* $^1$H NMR (300 MHz, $CD_3OD$): $\delta$ 8.87 (s, 1H), 7.87 (2s, 1H), 7.47−7.39 (m, 6H), 6.89−6.85 (m, 2H), 4.63 (s, 1H), 4.57−4.50 (m, 3H), 4.35 (d, $J$ = 15.3 Hz, 1H), 4.00−3.79 (m, 4H), 3.52−3.31 (m, 12H), 3.30−3.27 (m, 1H), 2.89−2.85 (2s, 3H), 2.48 (s, 3H), 2.28−2.04 (m, 9H), 1.85−1.74 (m, 7H), 1.63−1.54 (m, 8H), 1.39−1.37 (m, 2H), 1.04 (s, 9 H). LC-MS (ES$^+$): $m/z$ 1104.10 and 1106.10 [M + H$^+$].

*(2S,4R)-1-[(2S)-2-(1-{4-[(5-Bromo-4-{[3-(1-cyclobutyl-N-methylformamido)propyl]amino}pyrimidin-2-yl)amino]phenyl}-1,4,9,14,17-pentaoxanonadecan-19-amido)-3,3-dimethylbutanoyl]-4-hydroxy-N-{[4-(4-methyl-1,3-thiazol-5-yl)phenyl]methyl}-pyrrolidine-2-carboxamide (**3l**).* $^1$H NMR (300 MHz, $CD_3OD$): $\delta$ 8.87 (s, 1H), 7.87 (2s, 1H), 7.49−7.39 (m, 6H), 6.91−6.88 (m, 2H), 4.69 (s, 1H), 4.61−4.50 (m, 3H), 4.37−4.32 (m, 1H), 4.09−4.03 (m, 4H), 3.90−3.31 (m, 21H), 3.27−3.24 (m, 1H), 2.90−2.85 (2s, 3H), 2.47 (s, 3H), 2.25−1.97 (m, 6H), 1.86−1.77 (m, 3H), 1.62 (br, 8H), 1.04 (s, 9H). LC-MS (ES$^+$): $m/z$ 1136.10 and 1138.10 [M + H$^+$].

*(2S,4R)-1-[(2S)-2-(1-{4-[(5-bromo-4-{[3-(1-cyclobutyl-N-methylformamido)propyl]amino}pyrimidin-2-yl)amino]phenyl}-1,5,9,13,17-pentaoxaicosan-20-amido)-3,3-dimethylbutanoyl]-4-hydroxy-N-{[4-(4-methyl-1,3-thiazol-5-yl)phenyl]methyl}-pyrrolidine-2-carboxamide (**3m**).* $^1$H NMR (300 MHz, $CD_3OD$): $\delta$ 8.87 (s, 1 H), 7.87 (2s, 1H), 7.48−7.39 (m, 6H), 6.89−6.85 (m, 2H), 4.66−4.52 (m, 4H), 4.37 (m, 1H), 4.06−4.02 (m, 2H), 3.87−3.58 (m, 6H), 3.54−3.42 (m, 16H), 3.32−3.30 (m, 1H), 2.90−2.85 (2s, 3 H), 2.48−2.47 (m, 5H), 2.25−1.98 (m, 8H), 1.84−1.72 (m, 10H), 1.03 (s, 9 H). LC-MS (ES$^+$): $m/z$ 1150.1 and 1152.1 [M + H$^+$].

*(2S,4R)-1-[(2S)-2-(1-{4-[(5-Bromo-4-{[3-(1-cyclobutyl-N-methylformamido)propyl]amino}pyrimidin-2-yl)amino]phenyl}-1,4,7,12,17,20-hexaoxadocosan-22-amido)-3,3-dimethylbutanoyl]-4-hydroxy-N-{[4-(4-methyl-1,3-thiazol-5-yl)phenyl]methyl}-pyrrolidine-2-carboxamide (**3o**).* $^1$H NMR (300 MHz, $CD_3OD$): $\delta$ 8.87 (s, 1H), 7.87 (2s, 1H), 7.49−7.39 (m, 6H), 6.90 (d, $J$ = 11.7 Hz, 2H), 4.69 (s, 1 H), 4.58−4.52 (m, 3 H), 4.37 (m, 1 H), 4.12 (m, 2H), 4.02 (br s, 2H), 3.86−3.81 (m, 4H), 3.70−3.50 (m, 8H), 3.49−3.35 (m, 12H), 3.32−3.31 (m, 1H), 2.90−2.85 (2s, 3 H), 2.48 (s, 3H), 2.22−1.81 (m, 10H), 1.61−1.58 (br, 8H), 1.04 (s, 9 H). LC-MS (ES$^+$): $m/z$ 1180.2 and 1182.2 [M + H$^+$].

*(2S,4R)-1-[(2S)-2-(1-{4-[(5-Bromo-4-{[3-(1-cyclobutyl-N-methylformamido)propyl]amino}pyrimidin-2-yl)amino]phenyl}-1,7,12,17,22,28-hexaoxatriacontan-30-amido)-3,3-dimethylbutanoyl]-4-hydroxy-N-{[4-(4-methyl-1,3-thiazol-5-yl)phenyl]methyl}-pyrrolidine-2-carboxamide (**3p**).* $^1$H NMR (400 MHz, $CD_3OD$): $\delta$ 8.89 (s, 1H), 7.91 (br, 1H), 7.48−7.42 (m, 6H), 6.90−6.86 (m, 2H), 4.71 (s, 1H), 4.63−4.51 (m, 3H), 4.41−4.36 (m, 1H), 4.03−3.95 (m, 4H), 3.94−3.79 (m, 2H), 3.56 (t, $J$ = 6.0 Hz, 2H), 3.49−3.37 (m, 20H), 3.32−3.27 (m, 1H), 2.91 (s, 2H), 2.86 (s, 1H), 2.50 (s, 3H), 2.29−2.25 (m, 4H), 2.20−1.98 (m, 3H), 1.94−1.75 (m, 5H), 1.74−1.58 (m, 20H), 1.57−1.43 (m, 2H), 1.34−1.32 (m, 1H), 1.06 (s, 9H). LC-MS (ES$^+$): $m/z$ 1292.7 and 1294.7 [M + H$^+$].

*(2S,4S)-1-[(2S)-2-(1-{4-[(5-Bromo-4-{[3-(1-cyclobutyl-N-methylformamido)propyl]amino}pyrimidin-2-yl)amino]phenyl}-1,5,10,14-tetraoxahexadecan-16-amido)-3,3-dimethylbutanoyl]-4-hydroxy-N-{[4-(4-methyl-1,3-thiazol-5-yl)phenyl]methyl}-pyrrolidine-2-carboxamide (**4**).* This compound was prepared using a procedure similar to that for compound **3i**. $^1$H NMR (400 MHz, $CD_3OD$): $\delta$ 8.88 (s, 1H), 7.87 (2s, 1H), 7.49−7.40 (m, 6H), 6.90−6.86 (m, 2H), 4.63 (s, 1H), 4.58−4.54 (m, 2H), 4.39−4.35 (m, 2H), 4.06−3.96 (m, 5H), 3.75−3.70 (m, 1H), 3.63−3.52 (m, 4H), 3.50−3.42 (m, 11H), 3.32−3.28 (m, 1H), 2.91 (s, 2H), 2.86 (s, 1H), 2.49−2.48 (m, 4H), 2.25−2.10 (m, 3H), 2.02−1.99 (m, 4H), 1.89−1.82 (m, 5H), 1.63−1.60 (m, 4H), 1.05 (s, 9H). LC-MS (ES$^+$): $m/z$ 1091.8, 1093.8 [M + H$^+$].

*(2S,4R)-1-[(2S)-2-(1-{4-[(4-{[3-(1-Cyclobutyl-N-methylformamido)propyl]amino}pyrimidin-2-yl)amino]phenyl}-1,5,10,14-tetraoxahexadecan-16-amido)-3,3-dimethylbutanoyl]-4-hydroxy-N-{[4-(4-methyl-1,3-thiazol-5-yl)phenyl]methyl}-pyrrolidine-2-carboxamide (**5a**).* A solution of **20i** (1.0 g, 2.11 mmol) in dichloromethane (10 mL) and trifluoroacetic acid (5.0 mL) was stirred at rt for 3 h. The resulting mixture was concentrated under reduced pressure to give the corresponding carboxylic acid as a light yellow oil (884 mg). This oil (884 mg, 2.11 mmol) was mixed with **18f** (1.18 g, 2.74 mmol) and DIPEA (1.36 g, 10.5 mmol) in *N*,*N*-dimethylformamide (10 mL), and HATU (962 mg, 2.53 mmol) was added at 0 °C. The resulting mixture was stirred at rt for 2 h. The mixture was diluted with water (50 mL) and extracted with ethyl acetate (50 mL × 3). The combined organic layers were washed with brine (50 mL × 3), dried over anhydrous sodium sulfate, and evaporated under reduced pressure. The residue was purified by silica gel column chromatography using dichloromethane/methanol (10/1) as eluent to give **28** as a pale yellow oil (1.0 g, 57% yield). This oil (100 mg, 0.12 mmol) was mixed with *N*-[3-([2-[(4-hydroxyphenyl)-amino]pyrimidin-4-yl]amino)propyl]-*N*-methylcyclobutanecarboxamide (**29a**, 43 mg, 0.12 mmol, prepared from the hydrogenation of **10** in the presence of palladium on carbon) and cesium carbonate (78 mg, 0.24 mmol) in *N*,*N*-dimethylformamide (5 mL), and the mixture was stirred at 80 °C for 5 h. The resulting solution was diluted with water (30 mL) and extracted with ethyl acetate (50 mL × 3). The combined organic layers were washed with brine (50 mL × 3), dried over anhydrous sodium sulfate, and concentrated under reduced pressure. The residue was purified by preparative HPLC (XBridge Shield RP18 OBD Column, 5 $\mu$m, 19 × 150 mm; mobile phase, water with 10 mmol/L ammonium bicarbonate and acetonitrile, held in 73.0% acetonitrile for 11 min; detector, UV 254 nm) to afford **5a** as an off-white solid (26 mg, 21% yield). $^1$H NMR (400 MHz, $CD_3OD$): $\delta$ 8.88 (s, 1H), 7.70−7.60 (m, 1H), 7.47−7.39 (m, 6H), 6.86−6.84 (m, 2H), 5.88−5.80 (m, 1H), 4.68 (s, 1H), 4.60−4.52 (m, 3H), 4.35−4.30 (m, 1H), 4.03−4.02 (m, 2H), 3.96−3.94 (d, $J$ = 4.4 Hz, 2H), 3.87−3.80 (m, 2H), 3.61−3.50 (m, 5H), 3.44−3.29 (m, 9H), 2.90 (s, 2H), 2.85 (s, 1H), 2.47 (s, 3H), 2.25−2.10 (m, 4H), 2.00−1.96 (m, 5H), 1.86−1.80 (m, 6H), 1.60−1.57 (m, 4H), 1.03 (s, 9H). LC-MS (ES$^+$): $m/z$ 1014.2 [M + H$^+$].

*(2S,4R)-1-[(2S)-2-(1-{4-[(4-{[3-(1-Cyclobutyl-N-methylformamido)propyl]amino}-5-fluoropyrimidin-2-yl)amino]-phenyl}-1,5,10,14-tetraoxahexadecan-16-amido)-3,3-dimethylbutanoyl]-4-hydroxy-N-{[4-(4-methyl-1,3-thiazol-5-yl)phenyl]methyl}-pyrrolidine-2-carboxamide (**5b**).* This compound was prepared according to the procedure for **5a**. $^1$H NMR (400 MHz, $CD_3OD$): $\delta$ 8.88 (s, 1H), 7.65−7.64 (2s, 1H), 7.48−7.41 (m, 6H), 6.88−6.85 (m, 2H), 4.71 (s, 1H), 4.60−4.54 (m, 3H), 4.38−4.34 (m, 1H), 4.05−4.02 (m, 2H), 3.98−3.97 (d, $J$ = 4.4 Hz, 2H), 3.87−3.80 (m, 2H), 3.64−3.53 (m, 4H), 3.48−3.42 (m, 10H), 3.33−3.32 (m, 1H), 2.92 (s, 2H), 2.87 (s, 1H), 2.49 (s, 3H), 2.25−2.19 (m, 4H), 2.03−1.85 (m, 10H), 1.63−1.60 (m, 4H), 1.05 (s, 9H). LC-MS (ES$^+$): $m/z$ 1032.1 [M + H$^+$].

*(2S,4R)-1-[(2S)-2-(1-{4-[(5-Chloro-4-{[3-(1-cyclobutyl-N-methylformamido)propyl]amino}pyrimidin-2-yl)amino]phenyl}-1,5,10,14-tetraoxahexadecan-16-amido)-3,3-dimethylbutanoyl]-4-*


DOI: 10.1021/acs.jmedchem.7b00635
J. Med. Chem. 2018, 61, 583−598

*hydroxy-N-{[4-(4-methyl-1,3-thiazol-5-yl)phenyl]methyl}-pyrrolidine-2-carboxamide (**5c**).* $^1$H NMR (400 MHz, $CD_3OD$): $\delta$ 8.88 (s, 1H), 7.80−7.77 (2s, 1H), 7.49−7.41 (m, 6H), 6.90−6.86 (m, 2H), 4.71 (s, 1H), 4.58−4.54 (m, 3H), 4.37 (s, 1H), 4.06−4.03 (m, 2H), 3.98−3.97 (d, $J$ = 4.8 Hz, 2H), 3.87−3.80 (m, 2H), 3.62−3.51 (m, 4H), 3.50−3.32 (m, 10H), 3.29−3.20 (m, 1H), 2.91 (s, 2H), 2.86 (s, 1H), 2.49 (s, 3H), 2.26−1.99 (m, 9H), 1.89−1.83 (m, 5H), 1.63−1.60 (m, 4H), 1.05 (s, 9H). LC-MS (ES$^+$): $m/z$ 1048.1, 1050.1 [M + H$^+$].

*(2S,4R)-1-[(2S)-2-(1-{4-[(4-{[3-(1-Cyclobutyl-N-methylformamido)propyl]amino}-5-iodopyrimidin-2-yl)amino]-phenyl}-1,5,10,14-tetraoxahexadecan-16-amido)-3,3-dimethylbutanoyl]-4-hydroxy-N-{[4-(4-methyl-1,3-thiazol-5-yl)phenyl]methyl}-pyrrolidine-2-carboxamide (**5d**).* $^1$H NMR (400 MHz, $CD_3OD$): $\delta$ 8.88 (s, 1H), 8.02 (2s, 1H), 7.48−7.40 (m, 6H), 6.89−6.86 (m, 2H), 4.71 (s, 1H), 4.60−4.53 (m, 3H), 4.37 (s, 1H), 4.06−4.03 (m, 2H), 3.97−3.87 (m, 4H), 3.62−3.50 (m, 4H), 3.48−3.32 (m, 10H), 3.30−3.20 (m, 1H), 2.90 (s, 2H), 2.85 (s, 1H), 2.49 (s, 3H), 2.24−1.99 (m, 9H), 1.88−1.81 (m, 5H), 1.62−1.59 (m, 4H), 1.05 (s, 9H). LC-MS (ES$^+$): $m/z$ 1140.4 [M + H$^+$].

*(2S,4R)-1-[(2S)-2-(1-{4-[(4-{[3-(1-Cyclobutyl-N-methylformamido)propyl]amino}-5-(trifluoromethyl)pyrimidin-2-yl)amino]phenyl}-1,5,10,14-tetraoxahexadecan-16-amido)-3,3-dimethylbutanoyl]-4-hydroxy-N-{[4-(4-methyl-1,3-thiazol-5-yl)-phenyl]methyl}pyrrolidine-2-carboxamide (**5e**).* $^1$H NMR (400 MHz, $CD_3OD$): $\delta$ 8.88 (s, 1H), 8.02 (2s, 1H), 7.51−7.41 (m, 6H), 6.92−6.89 (m, 2H), 4.71 (s, 1H), 4.58−4.50 (m, 3H), 4.38 (s, 1H), 4.07−4.05 (m, 2H), 3.98−3.80 (m, 4H), 3.63−3.59 (m, 4H), 3.53−3.32 (m, 10H), 3.30−3.20 (m, 1H), 2.89 (s, 2H), 2.84 (s, 1H), 2.48 (s, 3H), 2.24−1.99 (m, 9H), 1.89−1.81 (m, 5H), 1.63−1.60 (m, 4H), 1.05 (s, 9H). LC-MS (ES$^+$): $m/z$ 1083.1 [M + H$^+$].

*(2S,4R)-1-[(2S)-2-(1-{4-[(4-{[3-(1-Cyclobutyl-N-methylformamido)propyl]amino}-5-methylpyrimidin-2-yl)amino]-phenyl}-1,5,10,14-tetraoxahexadecan-16-amido)-3,3-dimethylbutanoyl]-4-hydroxy-N-{[4-(4-methyl-1,3-thiazol-5-yl)phenyl]methyl}-pyrrolidine-2-carboxamide (**5f**).* $^1$H NMR (400 MHz, $CD_3OD$): $\delta$ 1.04 (s, 9H), 1.61−1.65 (m, 4H), 1.77−2.28 (m, 18H), 2.49 (s, 3H), 2.86−2.92 (2s, 3H), 3.38−3.65 (m, 14H), 3.80−4.10 (m, 6H), 4.35−4.71 (m, 5H), 6.94−6.98 (m, 2H), 7.38−7.52 (m, 7H), 8.90 (s, 1H). LC-MS (ES$^+$): $m/z$ 1028.3 [M + H$^+$].

*(2S,4R)-1-[(2S)-2-(1-{4-[(4-{[3-(1-Cyclobutyl-N-methylformamido)propyl]amino}-5-ethylpyrimidin-2-yl)amino]-phenyl}-1,5,10,14-tetraoxahexadecan-16-amido)-3,3-dimethylbutanoyl]-4-hydroxy-N-{[4-(4-methyl-1,3-thiazol-5-yl)phenyl]methyl}-pyrrolidine-2-carboxamide (**5g**).* $^1$H NMR (400 MHz, $CD_3OD$): $\delta$ 1.04 (s, 9H), 1.21−1.26 (m, 3H), 1.61−1.63 (m, 4H), 1.84−2.28 (m, 15H), 2.43−2.50 (m, 5H), 2.86−2.92 (2s, 3H), 3.41−3.65 (m, 14H), 3.80−3.91 (m, 2H), 3.94−4.03 (m, 2H), 4.07−4.12 (m, 2H), 4.35−4.40 (m, 1H), 4.49−4.62 (m, 3H), 4.71−4.80 (m, 1H), 6.98−7.00 (m, 2H), 7.36−7.49 (m, 7H), 8.89 (s, 1H). LC-MS (ES$^+$): $m/z$ 1043.1 [M + H$^+$].

*(2S,4R)-1-[(2S)-2-(1-{4-[(5-Cyclobutyl-4-{[3-(1-cyclobutyl-N-methylformamido)propyl]amino}pyrimidin-2-yl)amino]phenyl}-1,5,10,14-tetraoxahexadecan-16-amido)-3,3-dimethylbutanoyl]-4-hydroxy-N-{[4-(4-methyl-1,3-thiazol-5-yl)phenyl]methyl}-pyrrolidine-2-carboxamide (**5h**).* A mixture of *N*-[3-[(5-bromo-2-chloropyrimidin-4-yl)amino]propyl]-*N*-methylcyclobutanecarboxamide (**9**, 360 mg, 1.00 mmol), cyclobutylboronic acid (300 mg, 3.00 mmol), sodium carbonate (212.0 mg, 2.00 mmol), and 1,1′-bis(diphenylphosphino)ferrocene-palladium(II)dichloride dichloromethane complex (73 mg, 0.10 mmol) in toluene/water (5/1) (10 mL) was stirred at 100 °C under nitrogen atmosphere for 3 h. The resulting solution was extracted with ethyl acetate (50 mL × 3), and the combined organic layers were washed with brine (50 mL × 3) and dried over anhydrous sodium sulfate. The residue was purified by silica gel column chromatography using ethyl acetate/petroleum ether (1/1) as eluent to give *N*-[3-[(5-cyclobutyl-2-chloropyrimidin-4-yl)amino]-propyl]-*N*-methylcyclobutanecarboxamide as a light-yellow oil (100 mg, 30% yield). LC-MS (ES$^+$): $m/z$ 337.1, 339.1 [M + H$^+$]. This oily material (90 mg, 0.27 mmol) was mixed with 4-aminophenol (58 mg, 0.54 mmol) and 4-methylbenzenesulfonic acid (23 mg, 0.13 mmol) in dioxane (10 mL), and the mixture was stirred at 90 °C overnight. The resulting solution was diluted with water (20 mL) and extracted with ethyl acetate (50 mL × 3). The combined organic layers were washed with brine (50 mL × 3) and dried over anhydrous sodium sulfate. The residue was purified by silica gel column chromatography using ethyl acetate/petroleum ether (9/1) as eluent to provide *N*-[3-({5-cyclobutyl-2-[(4-hydroxyphenyl)amino]pyrimidin-4-yl}amino)-propyl]-*N*-methylcyclobutanecarboxamide as a black oil (70.0 mg, 64% yield). This material was used for the preparation of **5h** with the same method as that described for **5a**. $^1$H NMR (400 MHz, $CD_3OD$): $\delta$ 8.88 (s, 1H), 7.64 (2s, 1H), 7.49−7.46 (m, 4H), 7.43−7.41 (d, $J$ = 8.0 Hz, 2H), 6.88−6.85 (m, 2H), 4.71 (s, 1H), 4.60−4.50 (m, 3H), 4.38 (m, 1H), 4.05−3.97 (m, 4H), 3.95−3.75 (m, 2H), 3.63−3.59 (m, 7H), 3.53−3.41 (m, 8H), 3.30−3.20 (m, 1H), 2.91 (s, 2H), 2.85 (s, 1H), 2.49 (s, 3H), 2.48−2.40 (m, 2H), 2.25−1.98 (m, 12H), 1.79−1.90 (m, 6H), 1.63−1.60 (m, 4H), 1.05 (s, 9H). LC-MS (ES$^+$): $m/z$ 1068.4 [M + H$^+$].

*(2S,4R)-1-[(2S)-2-(1-{4-[(4-{[3-(1-Cyclobutyl-N-methylformamido)propyl]amino}-5-ethenylpyrimidin-2-yl)amino]-phenyl}-1,5,10,14-tetraoxahexadecan-16-amido)-3,3-dimethylbutanoyl]-4-hydroxy-N-{[4-(4-methyl-1,3-thiazol-5-yl)phenyl]methyl}-pyrrolidine-2-carboxamide (**5i**).* $^1$H NMR (400 MHz, $CD_3OD$): $\delta$ 1.04 (s, 9H), 1.60−1.63 (m, 4H), 1.80−2.28 (m, 15H), 2.49 (s, 3H), 2.85−2.91 (2s, 3H), 3.40−3.65 (m, 14H), 3.80−4.08 (m, 6H), 4.34−4.40 (m, 1H), 4.49−4.62 (m, 3H), 4.71 (s, 1H), 5.22−5.28 (m, 1H), 5.51−5.60 (m, 1H), 6.59−6.66 (m, 1H), 6.90−6.93 (m, 2H), 7.41−7.50 (m, 6H), 7.82−7.88 (2s, 1H), 8.89 (s, 1H). LC-MS (ES$^+$): $m/z$ 1040.56 1041.0 [M + H$^+$].

*(2S,4R)-1-[(2S)-2-(1-{4-[(4-{[3-(1-Cyclobutyl-N-methylformamido)propyl]amino}-5-cyclopropylpyrimidin-2-yl)-amino]phenyl}-1,5,10,14-tetraoxahexadecan-16-amido)-3,3-dimethylbutanoyl]-4-hydroxy-N-{[4-(4-methyl-1,3-thiazol-5-yl)phenyl]-methyl}pyrrolidine-2-carboxamide (**5j**).* $^1$H NMR (400 MHz, $CD_3OD$): $\delta$ 0.57−0.59 (m, 2H), 1.01−1.05 (m, 11H), 1.61−1.63 (m, 5H), 1.84−2.26 (m, 15H), 2.49 (s, 3H), 2.87, 2.94 (2s, 3H), 3.45−3.65 (m, 14H), 3.80−3.99 (m, 4H), 4.09 (t, $J$ = 6.2 Hz, 2H), 4.35−4.39 (m, 1H), 4.54−4.71 (m, 4H), 6.98−7.01 (m, 2H), 7.35−7.49 (m, 7H), 8.89 (s, 1H). LC-MS (ES$^+$): $m/z$ 1054.58 1054.9 [M + H$^+$].

**PROTACs 6a−e Prepared According to the Procedure for 3i.**

*(2S,4R)-1-[2-(1-{4-[(5-Bromo-4-{[3-(1-cyclobutyl-N-methylformamido)propyl]amino}pyrimidin-2-yl)amino]phenyl}-1,5,10,14-tetraoxahexadecan-16-amido)acetyl]-4-hydroxy-N-{[4-(4-methyl-1,3-thiazol-5-yl)phenyl]methyl}pyrrolidine-2-carboxamide (**6a**).* $^1$H NMR (400 MHz, $CD_3OD$): $\delta$ 8.87 (s, 1H), 7.88 and 7.85 (2s, 1H), 7.41−7.47 (m, 6H), 6.88 (dd, $J$ = 8.8 Hz, 1.8 Hz, 2H), 4.58 (t, $J$ = 7.9 Hz, 1H), 4.36−4.54 (m, 4H), 4.11−4.19 (m, 1H), 4.01−4.08 (m, 3H), 3.96 (d, $J$ = 2.0 Hz, 2H), 3.76 (dd, $J$ = 10.9 Hz, 4.2 Hz, 1H), 3.55−3.63 (m, 4H), 3.36−3.52 (m, 9H), 3.22−3.29 (m, 1H), 2.89 (s, 2H), 2.84 (s, 1H), 2.47 (s, 3H), 2.15−2.32 (m, 5H), 2.03−2.14 (m, 2H), 1.94−2.02 (m, 3H), 1.78−1.88 (m, 5H), 1.54−1.63 (m, 4H). LC-MS (ES$^+$): $m/z$ 1036.3, 1038.3 [M + H$^+$].

*(2S,4R)-1-[(2S)-2-(1-{4-[(5-Bromo-4-{[3-(1-cyclobutyl-N-methylformamido)propyl]amino}pyrimidin-2-yl)amino]phenyl}-1,5,10,14-tetraoxahexadecan-16-amido)propanoyl]-4-hydroxy-N-{[4-(4-methyl-1,3-thiazol-5-yl)phenyl]methyl}pyrrolidine-2-carboxamide (**6b**).* $^1$H NMR (400 MHz, $CD_3OD$): $\delta$ 8.87 (s, 1H), 7.88 and 7.85 (2s, 1 H), 7.31−7.54 (m, 6H), 6.89 (d, $J$ = 9.00 Hz, 2H), 4.74 (q, $J$ = 6.98 Hz, 1H), 4.55−4.64 (m, 1H), 4.35−4.54 (m, 3H), 4.04 (t, $J$ = 6.16 Hz, 2H), 3.90−3.97 (m, 2H), 3.73−3.82 (m, 2H), 3.55−3.64 (m, 4H), 3.38−3.54 (m, 9H), 3.22−3.29 (m, 1H), 2.90 and 2.84 (2s, 3H), 2.48 (s, 3H), 2.13−2.29 (m, 5H), 1.94−2.11 (m, 5H), 1.76−1.90 (m, 5H), 1.56−1.63 (m, 4H), 1.32 (d, $J$ = 6.5 Hz, 3H). LC-MS (ES$^+$): $m/z$ 1050.3, 1052.3 [M + H$^+$].

*(2S,4R)-1-[(2S)-2-(1-{4-[(5-Bromo-4-{[3-(1-cyclobutyl-N-methylformamido)propyl]amino}pyrimidin-2-yl)amino]phenyl}-1,5,10,14-tetraoxahexadecan-16-amido)butanoyl]-4-hydroxy-N-{[4-(4-methyl-1,3-thiazol-5-yl)phenyl]methyl}pyrrolidine-2-carboxamide (**6c**).* $^1$H NMR (400 MHz, $CD_3OD$): $\delta$ 8.87 (s, 1H), 7.88 and 7.86 (2s, 1H), 7.37−7.48 (m, 6H), 6.89 (d, $J$ = 9.0 Hz, 2H), 4.70 (dd, $J$ = 7.1, 5.6 Hz, 1H), 4.59 (t, $J$ = 8.2 Hz, 1H), 4.43−4.53 (m, 2H), 4.36−4.42 (m, 1H), 4.04 (t, $J$ = 6.3 Hz, 2H), 3.92−3.98 (m, 2H), 3.79 (d, $J$ = 2.5 Hz, 2H), 3.56−3.64 (m, 4H), 3.47−3.55 (m, 3H), 3.37−3.47 (m,


DOI: 10.1021/acs.jmedchem.7b00635
J. Med. Chem. 2018, 61, 583−598

6H), 3.19−3.29 (m, 1H), 2.90 (s, 2H), 2.84 (s, 1H), 2.48 (s, 3H), 2.14−2.30 (m, 5H), 1.96−2.12 (m, 5H), 1.65−1.95 (m, 7H), 1.59 (dt, $J$ = 5.8, 3.0 Hz, 4H), 0.93−0.97 (t, $J$ = 7.0 Hz, 3H). LC-MS ($ES^+$): $m/z$ 1064.3, 1066.3 [M + $H^+$].

*(2S,4R)-1-[(2S)-2-(1-{4-[(5-Bromo-4-{[3-(1-cyclobutyl-N-methylformamido)propyl]amino}pyrimidin-2-yl)amino]phenyl}-1,5,10,14-tetraoxahexadecan-16-amido)pentanoyl]-4-hydroxy-N-{[4-(4-methyl-1,3-thiazol-5-yl)phenyl]methyl}pyrrolidine-2-carboxamide (**6d**).* $^1$H NMR (400 MHz, $CD_3OD$): $\delta$ 8.87 (s, 1H), 7.89 and 7.86 (2s, 1H), 7.40−7.47 (m, 6H), 6.85−6.92 (m, 2H), 4.76 (dd, $J$ = 8.0, 4.9 Hz, 1H), 4.58 (t, $J$ = 8.2 Hz, 1H), 4.49 (d, $J$ = 15.5 Hz, 2H), 4.36−4.43 (m, 1H), 4.04 (t, $J$ = 6.2 Hz, 2H), 3.95 (d, $J$ = 2.2 Hz, 2H), 3.67−3.80 (m, 3H), 3.59 (t, $J$ = 6.3 Hz, 4H), 3.39−3.53 (m, 9H), 3.19−3.25 (m, 1H), 2.90 (s, 2H), 2.84 (s, 1H), 2.47 (s, 3H), 2.15−2.29 (m, 5H), 1.94−2.13 (m, 5H), 1.76−1.89 (m, 6H), 1.56−1.70 (m, 5H), 1.38 (m, 2H), 0.90−0.95 (m, 3H). LC-MS ($ES^+$): $m/z$ 1078.3, 1080.3 [M + $H^+$].

*(2S,4R)-1-[(2S)-2-(1-{4-[(5-Bromo-4-{[3-(1-cyclobutyl-N-methylformamido)propyl]amino}pyrimidin-2-yl)amino]phenyl}-1,5,10,14-tetraoxahexadecan-16-amido)-3-methylbutanoyl]-4-hydroxy-N-{[4-(4-methyl-1,3-thiazol-5-yl)phenyl]methyl}pyrrolidine-2-carboxamide (**6e**).* $^1$H NMR (400 MHz, $CD_3OD$): $\delta$ 8.87 (s, 1H), 7.88 and 7.85 (2s, 1H), 7.40−7.46 (m, 6H), 6.87−6.90 (m, 2H), 4.63 (d, $J$ = 6.7 Hz, 1H), 4.58 (t, $J$ = 8.3 Hz, 1H), 4.47−4.53 (m, 2H), 4.35−4.42 (m, 1H), 4.04 (t, $J$ = 6.2 Hz, 2H), 3.96 (d, $J$ = 4.9 Hz, 2H), 3.67−3.82 (m, 3H), 3.60 (m, 4H), 3.37−3.55 (m, 9H), 3.20−3.25 (m, 1H), 2.84 and 2.90 (2s, 3H), 2.47 (s, 3H), 2.13−2.28 (m, 6H), 2.03−2.12 (m, 2H), 1.96−2.03 (m, 3H), 1.75−1.88 (m, 5H), 1.59 (td, $J$ = 3.0, 5.8 Hz, 4H), 1.01 (d, $J$ = 6.8 Hz, 3H), 0.92 (d, $J$ = 6.8 Hz, 3H). LC-MS ($ES^+$): $m/z$ 1078.3, 1080.3 [M + $H^+$].

*N-[3-[(5-Bromo-2-chloropyrimidin-4-yl)amino]propyl]-N-methylcyclobutanecarboxamide (**9**).* To a solution of cyclobutanecarboxylic acid (2.66 g, 26.6 mmol) in *N*,*N*-dimethylformamide (100 mL) were added DIPEA (6.86 g, 53.1 mmol) and HATU (12.1 g, 31.9 mmol). After stirring at 0−10 °C for 30 min, *tert*-butyl *N*-[3-(methylamino)-propyl]carbamate (5 g, 26.6 mmol) was added. The resulting solution was stirred at rt for 12 h. The reaction was quenched with water (500 mL) and extracted with ethyl acetate (3 × 100 mL). The combined organic layers were washed with water (100 mL) and brine (100 mL). The mixture was dried over anhydrous sodium sulfate and concentrated *in vacuo*. The residue was purified by silica gel column chromatography using ethyl acetate/petroleum ether (1:1) as eluent to afford *tert*-butyl *N*-[3-(1-cyclobutyl-*N*-methylformamido)propyl]-carbamate as a colorless oil (5.9 g, 82% yield). LC-MS ($ES^+$): $m/z$ 271.1 [M + $H^+$]. The oily material (13.0 g, 48.1 mmol) in methanol/HCl (g) (200 mL) was stirred at rt for 1 h. The resulting mixture was concentrated *in vacuo* to provide *N*-(3-aminopropyl)-*N*-methylcyclobutanecarboxamide hydrochloride (**8**) as a white solid (9.6 g, 97% yield). LC-MS ($ES^+$): $m/z$ 171.0 [M + $H^+$]. This hydrochloride salt (9.6 g, 46.4 mmol) was mixed with 5-bromo-2,4-dichloropyrimidine (10.5 g, 46.3 mmol) in acetonitrile (250 mL), and DIPEA (18.0 g, 139.3 mmol) was added at 0 °C. The resulting solution was slowly warmed to rt and stirred for 3 h. The reaction was quenched with water (50 mL) and extracted with ethyl acetate (3 × 100 mL). The combined organic layers were washed with brine (500 mL), dried over anhydrous sodium sulfate, and concentrated *in vacuo*. The residue was suspended in 200 mL of ethyl acetate/petroleum ether (1/5, v/v), and the white solid was collected by filtration (11.3 g, 67% yield). $^1$H NMR (400 MHz, $CDCl_3$) $\delta$ 8.09 (s, 1 H), 7.20 (b, 1 H), 3.49−3.47 (m, 4 H), 3.46−3.28 (m, 1 H), 2.93 (s, 3H), 2.41−2.31 (m, 2 H), 2.24−2.16 (m, 2 H), 2.05−1.80 (m, 2 H), 1.80−1.70 (m, 2 H). LC-MS ($ES^+$): $m/z$ 360.9 and 362.9 [M + $H^+$].

*N-[3-([5-Bromo-2-[(4-hydroxyphenyl)amino]pyrimidin-4-yl]-amino)propyl]-N-methylcyclobutanecarboxamide (**10**).* A solution of **9** (2.0 g, 5.56 mmol), 4-aminophenol (1.2 g, 11.0 mmol), and 4-methylbenzenesulfonic acid (480 mg, 2.79 mmol) in dioxane (30 mL) was stirred at 90 °C overnight. The pH value of the solution was adjusted to 7−8 with aqueous sodium bicarbonate solution, and the resulting solution was extracted with ethyl acetate (20 mL × 3). The combined organic layers were washed with brine (20 mL × 2), dried over anhydrous sodium sulfate, and concentrated. The residue was purified by silica gel column chromatography using ethyl acetate/petroleum ether (1:5) as eluent to afford **10** as a brown solid (1.52 g, 63% yield). $^1$H NMR (300 MHz, *d*-DMSO): $\delta$ 8.96 (2s, 1 H), 8.86 (s, 1 H), 7.93 (2s, 1 H), 7.44 (d, $J$ = 8.7 Hz, 2 H), 6.97−6.87 (m, 1 H), 6.66 (d, $J$ = 11.1 Hz, 2 H), 3.37−3.23 (m, 4 H), 3.20−3.15 (m, 1 H), 2.82 (s, 2 H), 2.75 (s, 1 H), 2.17−2.04 (m, 3 H), 1.98−1.67 (m, 5 H). LC-MS ($ES^+$): $m/z$ 434.1 and 436.1 [M + $H^+$].

*4-(4-Methylthiazol-5-yl)benzonitrile (**12**).* A mixture of 4-bromobenzonitrile (19.0 g, 104 mmol), 4-methylthiazole (21.0 g, 212 mmol), KOAc (20.5 g, 244 mmol), and $Pd(OAc)_2$ (700 mg, 3.1 mmol) in DMA (200 mL) was purged with $N_2$ at 0 °C for 10 min, then heated at 150 °C for 5 h. After cooling to rt, the mixture was quenched with water (1 L) and extracted with ethyl acetate (500 mL × 3). The combined organic layers were washed with brine (500 mL), dried over anhydrous sodium sulfate, and concentrated *in vacuo*. The residue was purified by silica gel column chromatography using ethyl acetate/petroleum ether (1:1) as eluent to afford **12** as a yellow solid (19.0 g, 91.3% yield). $^1$H NMR (400 MHz, $CDCl_3$): $\delta$ 8.77 (s, 1H), 7.73 (d, $J$ = 7.6 Hz, 2H), 7.57 (d, $J$ = 7.6 Hz, 2H), 2.57 (s, 3H). LC-MS ($ES^+$): $m/z$ 201.1 [M + $H^+$].

*(4-(4-Methylthiazol-5-yl)phenyl)methanamine (**13**).* To a solution of **12** (17 g, 85 mmol) in THF (300 mL) was added $LiAlH_4$ (6.34 g, 167 mmol) in batches at 0 °C. The resulting mixture was heated at 70 °C for 5 h. The reaction was quenched by 10% aqueous NaOH solution at 0 °C and stirred for 30 min. The mixture was filtered through a pad of Celite, and the filtered cake was washed with 10% $MeOH/CH_2Cl_2$ four times. The filtrate was concentrated under reduced pressure to afford the desired product **13** (11 g, 63.4% yield), which was used in the next step without further purification. $^1$H NMR (400 MHz, $CDCl_3$): $\delta$ 8.67 (s, 1H), 7.29−7.43 (m, 4H), 3.92 (s, 2H), 2.54 (s, 3H), 1.62 (br, 2H). LC-MS ($ES^+$): $m/z$ 205.1 [M + $H^+$].

*(2R,4R)-N-(4-(4-Methylthiazol-5-yl)benzyl)-4-hydroxypyrrolidine-2-carboxamide Hydrochloride (**16**).* To a solution of *trans*-*N*-Boc-4-hydroxyproline (**14**) (1.9 g, 8.2 mmol), **13** (1.7 g, 8.3 mmol), and DIPEA (5 mL) in DMF (10 mL) was added HATU (4.8 g, 12.6 mmol) at 0 °C. The resulting mixture was stirred at rt for 2 h and quenched with water. The mixture was extracted with ethyl acetate (50 mL × 3). The combined organic layers were washed with brine, dried over anhydrous $Na_2SO_4$, and concentrated. The residue was purified by silica gel column chromatography to afford (2*S*,4*R*)-*tert*-butyl 2-((4-(4-methylthiazol-5-yl)benzyl)carbamoyl)-4- hydroxypyrrolidine-1-carboxylate (**15**) as an off white solid (1.4 g, 40.8% yield). LC-MS ($ES^+$): $m/z$ 418.1 [M + $H^+$]. This material (1.4 g, 3.3 mmol) was dissolved in HCl in methanol (15 mL), and the solution was stirred at rt for 2 h. The solvent was evaporated under reduced pressure to provide **16** (800 mg), which was used in the next step without further purification. $^1$H NMR (400 MHz, $CD_3OD$): $\delta$ 9.73 (s, 1H), 9.01 (br s, 1H), 7.56 (d, $J$ = 7.2 Hz, 2H), 7.50 (d, $J$ = 7.6 Hz, 2H), 4.49−4.61 (m, 4H), 3.42−3.46 (m, 2H), 2.56 (s, 3H), 2.47−2.53 (m, 1H), 2.06−2.12 (m, 1H). LC-MS ($ES^+$): $m/z$ 318.1 [M + $H^+$].

*(2S,4R)-1-[(2S)-2-Aminopropanoyl]-4-hydroxy-N-{[4-(4-methyl-1,3-thiazol-5-yl)phenyl]methyl}pyrrolidine-2-carboxamide Hydrochloride (**18b**).* To a solution of (*tert*-butoxycarbonyl)-L-alanine (0.84 g, 4.2 mmol), DIPEA (2.44 g, 18.9 mmol), HATU (1.94 g, 5.1 mmol) in DMF (50 mL) was added **16** (1.5 g, 4.2 mmol). The resulting solution was stirred at rt for 3 h and quenched with water (100 mL). The mixture was extracted with ethyl acetate (100 mL × 2). The combined organic layers were washed with water and brine. The residue was purified by silica gel column chromatography to afford *tert*-butyl *N*-[(2*S*)-1-[(2*S*,4*R*)-4-hydroxy-2-({[4-(4-methyl-1,3-thiazol-5-yl)phenyl]methyl}carbamoyl)pyrrolidin-1-yl]-1-oxopropan-2-yl]-carbamate (**17b**) as an off white solid (1.45 g, 70% yield). $^1$H NMR (400 MHz, $CDCl_3$): $\delta$ 8.68 (s, 1H), 7.37−7.39 (m, 3H), 7.27−7.31 (m, 2H), 5.24 (d, $J$ = 7.2 Hz, 1H), 4.76 (t, $J$ = 7.2 Hz, 1H), 4.59 (br s, 1H), 4.37−4.54 (m, 3H), 3.96 (d, $J$ = 11.2 Hz, 1H), 3.02(s, 1H), 2.52−2.57 (m, 4H), 2.09−2.14 (m, 1H), 1.41 (s, 9H), 1.26 (m, 3H). LC-MS ($ES^+$) $m/z$ 489.2 [M + $H^+$]. This material (1.45 g, 2.97 mmol) in HCl/dioxane (20 mL) was stirred at rt for 3 h. The mixture was concentrated *in vacuo*, and the solid was washed with dichloromethane in petroleum ether (1:1) to afford the desired product **18b** as an off


DOI: 10.1021/acs.jmedchem.7b00635
J. Med. Chem. 2018, 61, 583−598

white solid (1.23 g, 98% yield). $^1$H NMR (400 MHz, $CD_3OD$): $\delta$ 10.07 (s, 1H), 7.56 (br s, 4H), 4.63 (t, $J$ = 8.4 Hz, 1H), 4.52−4.56 (m, 2H), 4.42−4.46 (m, 1H), 4.29−4.31 (m, 1H), 3.59−3.76 (m, 2H), 2.62 (s, 3H), 2.31−2.34 (m, 1H), 2.02−2.08 (m, 1H), 1.51 (d, $J$ = 7.2 Hz, 3H). LC-MS (ES$^+$): $m/z$ 389.2 [M + H$^+$].

**Intermediates 18a, 18c−f Prepared Using the Same Method As That Described in 18b.** *(2S,4R)-1-(2-Aminoacetyl)-4-hydroxy-N-{[4-(4-methyl-1,3-thiazol-5-yl)phenyl]methyl}pyrrolidine-2-carboxamide hydrochloride (**18a**).* $^1$H NMR (400 MHz, $CD_3OD$): $\delta$ 9.67 (br s, 1H), 7.52 (s, 4H), 4.53−4.61 (m, 3H), 4.40−4.44 (m, 1H), 3.72−3.96 (m, 4H), 2.57 (s, 3H), 2.20−2.30 (m, 1H), 2.07−2.11 (m, 1H). LC-MS (ES$^+$): $m/z$ 375.1 [MH$^+$].

*(2S,4R)-1-[(2S)-2-Aminobutanoyl]-4-hydroxy-N-{[4-(4-methyl-1,3-thiazol-5-yl)phenyl]methyl}pyrrolidine-2-carboxamide Hydrochloride (**18c**).* $^1$H NMR (400 MHz, $CD_3OD$): $\delta$: 9.85 (s, 1H), 7.54 (s, 4H), 4.64 (t, $J$ = 8.8 Hz, 1H), 4.42−4−55 (m, 3H), 4.24 (s, 1H), 3.72−3.78 (m, 2H), 2.59 (s, 3H), 2.28−2.33 (m, 1H), 2.06−2.09 (m, 1H), 1.91−1.96 (m, 2H), 1.05−1.07 (m, 3H). LC-MS (ES$^+$): $m/z$ 403.2 [M + H$^+$].

*(2S,4R)-1-[(2S)-2-Aminopentanoyl]-4-hydroxy-N-{[4-(4-methyl-1,3-thiazol-5-yl)phenyl]methyl}pyrrolidine-2-carboxamide Hydrochloride (**18d**).* $^1$H NMR (400 MHz, $CD_3OD$): $\delta$ 9.97 (s, 1H), 7.55 (s, 4H), 4.64 (t, $J$ = 8.8 Hz, 1H), 4.47−4.55 (m, 3H), 4.26 (s, 1H), 3.72 (m, 2H), 2.61 (s, 3H), 2.28−2.33 (m, 1H), 2.04−2.08 (m, 1H),1.80−1.89 (m, 2H), 1.52−1.58 (m, 2H), 1.00 (t, $J$ = 6.8 Hz, 3H). LC-MS (ES$^+$): $m/z$ 417.2 [M + H$^+$].

*(2S,4R)-1-[(2S)-2-Amino-3-methylbutanoyl]-4-hydroxy-N-{[4-(4-methyl-1,3-thiazol-5-yl)phenyl]methyl}pyrrolidine-2-carboxamide Hydrochloride (**18e**).* $^1$H NMR (400 MHz, $CD_3OD$): $\delta$ 9.97 (s, 1H), 7.55 (s, 4H), 4.42−4.67 (m, 4H), 4.13−4.14 (m, 1H), 3.66−3.75 (m, 2H), 2.61 (s, 3H), 2.29−2.34 (m, 2H), 2.03−2.10 (m, 1H), 1.14−1.18 (m, 6H). LC-MS (ES$^+$): $m/z$ 417.2 [M + H$^+$].

*(2S,4R)-1-[(2S)-2-Amino-3,3-dimethylbutanoyl]-4-hydroxy-N-{[4-(4-methyl-1,3-thiazol-5-yl)phenyl]methyl}pyrrolidine-2-carboxamide Hydrochloride (**18f**).* $^1$H NMR (400 MHz, $CD_3OD$): $\delta$ 9.84−9.82 (s, 1H), 7.58−7.54 (m, 4H), 4.71−4.41 (m, 4H), 4.13−4.08 (m, 1H), 3.86−3.71 (m, 2H), 2.60−2.58 (s, 3H), 2.35−2.07 (m, 2H), 1.19−1.12 (m, 9H). LC-MS (ES$^+$): $m/z$ 431.2 [M + H$^+$].

*tert-Butyl 2-(4-(tosyloxy)butoxy)acetate (**20a**).* A mixture of *tert*-butyl 2-(4-hydroxybutoxy)acetate (**19a**, 500 mg, 2.5 mmol), 4-toluenesulfonyl chloride (520 mg, 2.7 mmol), triethylamine (1.5 mL, 8.75 mmol), and DMAP (16 mg, 0.14 mmol) in dichloromethane (20 mL) was stirred at rt overnight. The reaction mixture was diluted with dichloromethane (50 mL) and washed with water and brine. The organic layer was dried over sodium sulfate, filtered, and concentrated. The residue was purified by silica gel column chromatography using 10−15% ethyl acetate in hexanes as eluent to afford **20a** as a colorless oil (700 mg, 87% yield). $^1$H NMR (400 MHz, $CDCl_3$): $\delta$ 1.47 (s, 9H), 1.62−1.67 (m, 2H), 1.75−1.82 (m, 2H), 2.45 (s, 3H), 3.47 (t, $J$ = 6.0 Hz, 2H), 3.89 (s, 2H), 4.07 (t, $J$ = 6.4 Hz, 2H), 7.34 (d, $J$ = 8.0 Hz, 2H), 7.78 (d, $J$ = 8.0 Hz, 2H).

*tert-Butyl 2-(4-(4-nitrophenoxy)butoxy)acetate (**21a**).* A mixture of 4-nitrophenol (240 mg, 1.7 mmol), **20a** (700 mg, 2.0 mmol), and $K_2CO_3$ (700 mg, 5.1 mmol) in DMF (5 mL) was stirred at 70 °C for 16 h. The mixture was partitioned between ethyl acetate and water. The organic phase was washed with brine, dried over anhydrous sodium sulfate, filtered, and concentrated. The residue was purified by silica gel column chromatography using 20−50% ethyl acetate in hexanes as eluent to provide **21a** as a light-yellow solid (600 mg, 90% yield). $^1$H NMR (400 MHz, $CDCl_3$): $\delta$ 1.50 (s, 9H), 1.80−1.87 (m, 2H), 1.95−2.03 (m, 2H), 3.62 (t, $J$ = 6.0 Hz, 2H), 3.99 (s, 2H), 4.14 (t, $J$ = 6.4 Hz, 2H), 6.97 (d, $J$ = 7.2 Hz, 2H), 8.21 (d, $J$ = 7.2 Hz, 2H). LC-MS (ES$^+$): $m/z$ 348.2 [M + Na$^+$].

*(2S,4S)-1-[(2S)-2-Amino-3,3-dimethylbutanoyl]-4-hydroxy-N-{[4-(4-methyl-1,3-thiazol-5-yl)phenyl]methyl}pyrrolidine-2-carboxamide Hydrochloride (**27**).* To a solution of *cis*-*N*-Boc-proline **24** (9.0 g, 38.9 mmol), **13** (8.0 g, 39.2 mmol), and DIPEA (8.0 g, 61.9 mmol) in DMF (100 mL) was added HATU (18.0 g, 47.4 mmol). The resulting mixture was stirred at rt overnight. The solution was diluted with water (200 mL) and extracted with ethyl acetate (300 mL × 3). The combined organic layers were washed with water (300 mL) and brine (300 mL), dried over anhydrous sodium sulfate, and concentrated under reduced pressure. The residue was purified by silica gel flash column chromatography to give a pale red oil (10 g, 61% yield). This oily material (10 g, 24.0 mmol) in HCl/MeOH (100 mL) was stirred at rt for 2 h. The resulting mixture was concentrated under reduced pressure to afford (2*S*,4*S*)-4-hydroxy-*N*-[[4-(4-methyl-1,3-thiazol-5-yl)phenyl]methyl]pyrrolidine-2-carboxamide hydrochloride (**25**) as a yellow solid (4.5 g, 53% yield). LC-MS (ES$^+$): $m/z$ 318.1 [M + H$^+$]. This solid (9.0 g, 25.4 mmol) was mixed with (2*S*)-2-[(*tert*-butoxy)carbonyl]amino-3,3-dimethylbutanoic acid (5.8 g, 25.1 mmol) and DIPEA (5.0 g, 38.7 mmol) in *N*,*N*-dimethylformamide (50 mL), and HATU (11.6 g, 30.5 mmol) was added at 0 °C. The resulting solution was stirred at rt for 16 h. The reaction mixture was diluted with water (200 mL) and extracted with ethyl acetate (300 mL × 3). The combined organic layers were washed with water (100 mL) and brine (100 mL), dried over anhydrous sodium sulfate, and concentrated under reduced pressure. The residue was purified by silica gel flash column chromatography using ethyl acetate/petroleum ether (10/90) as eluent to give *tert*-butyl *N*-[(2S)-1-[(2*S*,4*S*)-4-hydroxy-2-([[4-(4-methyl-1,3-thiazol-5-yl)phenyl]methyl]carbamoyl)-pyrrolidin-1-yl]-3,3-dimethyl-1-oxobutan-2-yl]carbamate (**26**) as a pale red oil (10 g, 74% yield). LC-MS (ES$^+$): $m/z$ 531.2 [M + H$^+$]. This oily material (10 g, 18.8 mmol) in HCl/MeOH (20 mL) was stirred at rt for 2 h. The resulting mixture was concentrated under reduced pressure to afford **27** as a yellow solid (6 g, 68% yield). $^1$H NMR (DMSO-$d_6$): $\delta$ 9.04 (s, 1H), 8.80−8.76 (m, 1H), 8.20 (br, 3H), 7.43−7.40 (m, 4H), 4.47−4.40 (m, 2H), 4.31−4.22 (m, 2H), 4.09−3.90 (m, 2H), 3.33−3.31 (m, 1H), 2.51 (s, 3H), 2.51−2.49 (m, 1H), 1.80−1.65 (m, 1H), 1.00 (s, 9H). LC-MS (ES$^+$): $m/z$ 431.2 [M + H$^+$].

**Western Blot Assay to Determine TBK1/IKK$\varepsilon$ Degradation and IRF3 Phosphorylation.** Panc02.13 cells were purchased from ATCC and cultured in RPMI-1640 (Gibco), supplemented with 15% FBS (ATCC) and 10 units/mL human recombinant insulin (Gibco). PROTAC treatments were carried out in 12-well plates for 16 h. TLR3 agonist Poly I:C (Invivogen; tlrl-pic) was added for the final 3 h. Cells were harvested and lysed in RIPA buffer (50 mM Tris at pH 8, 150 mM NaCl, 1% Tx-100, 0.1% SDS, and 0.5% sodium deoxycholate) supplemented with protease and phosphatase inhibitors. Lysates were clarified at 16,000*g* for 10 min, and supernatants were separated by SDS−PAGE. Immunoblotting was performed using standard protocols. The antibodies used were TBK1 (Cell Signaling#3504), pIRF3 (abcam#ab76493), and GAPDH (Cell Signaling#5174).

**Proliferation Assay.** The indicated lung cancer cell lines were plated in 50 $\mu$L in 96-well plates at 5000 cells/well. After 24 h, 50 $\mu$L of 2× drug solution (3-fold dilutions, 10 $\mu$M maximum concentration) was added for a final DMSO concentration of 0.1%, and plates were incubated for 72 h, following which 100 $\mu$L of CellTiterGlo reagent (Promega #G7570) was added to each well, and luminescence was measured.

**IKK$\varepsilon$ Knockdown.** Three unique Trilencer siRNA duplexes were purchased from Origene with the following sequence information: siRNA1, AGAUUCACAAGCUGGAUAAGGUGdAdA; siRNA2, ACCUUCAAGAAGUGGAAUAAAUGdUdG; siRNA3, GACAGAAAGCAUAACAUACACUCdGdC. The siRNA sequences were transfected into Panc02.13 cells in a 12-well plate using Lipofectamine RNAimax (Invitrogen) following the manufacturer's protocols. Cells were harvested 60 h after transfection and analyzed for protein levels by immunoblotting.

**TBK1 $K_d$ Determination.** Compounds were shipped as 10 mM DMSO stocks to DiscoverX (San Diego, CA) to evaluate $K_d$ values in duplicate against either TBK1 or IKK$\varepsilon$ in 12-point dose−response curves starting at the highest concentration of 10 $\mu$M.

**His-Tagged VHL Protein and Fluorescein-Labeled HIF-1$\alpha$ Peptide.** VHL was coexpressed and copurified with Elongin C and B (VCB) as previously described.[23] For the fluorescence polarization assay, a fluorescein labeled HIF-1$\alpha$ peptide (FAM-DEALA-Hyp-YIPD) was synthesized and purified as previously described.[24]

**VHL Binding Assay Based on Fluorescence Polarization.** Compounds were serially diluted in 100% DMSO and 2 $\mu$L transferred to Corning Costar 384-well black assay plates (Corning, #3575). To



DOI: 10.1021/acs.jmedchem.7b00635
J. Med. Chem. 2018, 61, 583−598

the assay plates, 8 μL of 2.5 μM VHL protein in buffer A (50 mM Tris pH7.5, 200 mM NaCl, 2 mM DTT and 1% DMSO) was added and incubated with the compound for 10 min. Next, 10 μL of 40 nM fluorescein labeled HIF-1α peptide (in buffer A) was added to each well to give a final peptide concentration of 20 nM and a final VHL concentration of 125 nM. Plates were incubated in the dark for 2 h. Fluorescence polarization from the assay plates was read using a Cytation3 plate reader equipped with a FP Green Cube (Biotek Instruments, Winooski, VT). FP Values were converted to percent binding based on control wells and $IC_{50}$ values calculated in GraphPad Prism using the four-parameter nonlinear regression dose−response model.

## ■ ASSOCIATED CONTENT

### Supporting Information

The Supporting Information is available free of charge on the ACS Publications website at DOI: 10.1021/acs.jmedchem.7b00635.

Synthetic procedures and related analytical data for the linker intermediates **19a−p** (PDF)

Biological data cited in Tables 1, 2, and 3 (CSV)

## ■ AUTHOR INFORMATION


### Corresponding Authors

*(A.P.C.) E-mail: andy.crew@arvinas.com.

*(C.M.C.) E-mail: craig.crews@yale.edu.

### ORCID

Craig M. Crews: 0000-0002-8456-2005

### Present Address

‖D.V.: Agios Pharmaceuticals, Cambridge, MA.


### Notes

The authors declare the following competing financial interest(s): C.M.C. is a consultant and shareholder of Arvinas, LLC, which supports research in his lab. A.P.C, K.R., H.D., Y.Q., J.W., B.D.H., A.M., C.F., T.N., and K.C. are shareholders and employees. D.V., K.S., and J.W. are Arvinas shareholders.

## ■ ACKNOWLEDGMENTS

We thank Suzhou Medinoah Co. Ltd. and Pharmaron for providing synthetic assistance. C.M.C. gratefully acknowledges support from the NIH (R35 CA197589).

## ■ ABBREVIATIONS USED

DIPEA, diisopropylethylamine; HATU, 1-[bis(dimethylamino)methylene]-1*H*-1,2,3-triazolo[4,5-*b*]pyridinium 3-oxide hexafluorophosphate; $DC_{50}$, half maximal degradation concentration; $D_{max}$, maximal degradation effect

## ■ REFERENCES


(1) Toure, M.; Crews, C. M. Small molecule PROTACs: new approaches to protein degradation. *Angew. Chem., Int. Ed.* **2016**, *55*, 1966−1973.

(2) Corson, T. W.; Aberle, N.; Crews, C. M. Design and applications of bifunctional small molecules: why two heads are better than one. *ACS Chem. Biol.* **2008**, *3*, 677−692.

(3) Sakamoto, K. M.; Kim, K. B.; Verma, R.; Ransick, A.; Stein, B.; Crews, C. M.; Deshaies, R. J. Development of PROTACs to target cancer-promoting proteins for ubiquitination and degradation. *Mol. Cell. Proteomics* **2003**, *2*, 1350−1358.

(4) Sakamoto, K. M.; Kim, K. B.; Kumagai, A.; Mercurio, F.; Crews, C. M.; Deshaies, R. J. PROTACs: chimeric molecules that target protein to the Skp1-Cullin-F box complex for ubiquitination and degradation. *Proc. Natl. Acad. Sci. U. S. A.* **2001**, *98*, 8554−8559.

(5) Lebraud, H.; Wright, D. J.; Johnson, C. N.; Heightman, T. D. Protein degradation by in-cell self-assembly of proteolysis targeting chimeras. *ACS Cent. Sci.* **2016**, *2* (12), 927−934.

(6) Schiedel, M.; Herp, D.; Hammelmann, S.; Swyter, S.; Lehotzky, A.; Robaa, D.; Olah, J.; Ovádi, J.; Sippl, W.; Jung, M. Chemically induced degradation of sirtuin 2 (Sirt2) by a proteolysis targeting chimera (PROTAC) based on sirtuin rearranging ligands (SirReals). *J. Med. Chem.*. DOI: 10.1021/acs.jmedchem.6b01872. Published online: Apr 5, **2017**. http://pubs.acs.org/doi/abs/10.1021/acs.jmedchem.6b01872 (accessed Apr 5, 2017).

(7) Schneekloth, J. S., Jr.; Fonseca, F. N.; Koldobskiy, M.; Mandal, A.; Deshaies, R.; Sakamoto, K.; Crews, C. M. Chemical genetic control of protein levels: selective in vivo targeted degradation. *J. Am. Chem. Soc.* **2004**, *126*, 3748−3754.

(8) Salami, J.; Crews, C. M. Waste disposal - An attractive strategy for cancer therapy. *Science* **2017**, *355*, 1163−1167.

(9) Schneekloth, A. R.; Pucheault, M.; Tae, H. S.; Crews, C. M. Targeted intracellular protein degradation induced by a small molecule: en route to chemical proteomics. *Bioorg. Med. Chem. Lett.* **2008**, *18*, 5904−5908.

(10) (a) Doak, B. C.; Over, B.; Giordanetto, F.; Kihlberg, J. Oral druggable space beyond the rule of 5: insights from drugs and clinical candidates. *Chem. Biol.* **2014**, *21*, 1115−1142. (b) Doak, B. D.; Zheng, J.; Dobritzsch, D.; Kihlberg, J. How beyond rule of 5 drugs and clinical candidates bind to their targets. *J. Med. Chem.* **2016**, *59*, 2312−2327.

(11) Ottis, P.; Crews, C. M. PROTACs: induced protein degradation as a therapeutic strategy. *ACS Chem. Biol.* **2017**, *12*, 892−898.

(12) (a) Lu, J.; Qian, Y.; Altieri, M.; Dong, H.; Wang, J.; Raina, K.; Hines, J.; Winkler, J. D.; Crew, A. P.; Coleman, K.; Crews, C. M. Hijacking the E3 ubiquitin ligase cereblon to efficiently target BRD4. *Chem. Biol.* **2015**, *22*, 755−763. (b) Raina, K.; Lu, J.; Qian, Y.; Altieri, M.; Gordon, D.; Rossi, A. M. K.; Wang, J.; Chen, X.; Dong, H.; Siu, K.; Winkler, J. D.; Crew, A. P.; Crews, C. M.; Coleman, K. G. PROTAC-induced BET protein degradation as a therapy for castration-resistant prostate cancer. *Proc. Natl. Acad. Sci. U. S. A.* **2016**, *113*, 7124−7129. (c) Saenz, D. T.; Fiskus, W.; Qian, Y.; Manshouri, T.; Rajapakshe, K.; Raina, K.; Coleman, K. G.; Crew, A. P.; Shen, A.; Mill, C. P.; Sun, B.; Qiu, P.; Kadia, T. M.; Pemmaraju, N.; DiNardo, C.; Kim, M.-S.; Nowak, A. J.; Coarfa, C.; Crews, C. M.; Verstovsek, S.; Bhalla, K. N. Novel BET protein proteolysis-targeting chimera exerts superior lethal activity than bromodomain inhibitor (BETi) against post-myeloproliferative neoplasm secondary (s) AML cells. *Leukemia*. DOI: 10.1038/leu.2016.393. Published online: Jan 2, **2017**. http://www.nature.com/leu/journal/vaop/ncurrent/full/leu2016393a.html (accessed Jan 2, 2017).

(13) Bondeson, D. P.; Mares, A.; Smith, I. E.D.; Ko, E.; Campos, S.; Miah, A. H.; Mulholland, K. E.; Routly, N.; Buckley, D. L.; Gustafson, J. L.; Zinn, N.; Grandi, P.; Shimamura, S.; Bergamini, G.; Faelth-Savitski, M.; Bantscheff, M.; Cox, C.; Gordon, D. A.; Willard, R. R.; Flanagan, J. J.; Casillas, L. N.; Votta, B. J.; den Besten, W.; Famm, K.; Kruidenier, L.; Carter, P. S.; Harling, J. D.; Churcher, I.; Crews, C. M. Catalytic *in vivo* protein knockdown by small-molecule PROTACs. *Nat. Chem. Biol.* **2015**, *11*, 611−617.

(14) (a) Clark, K.; Plater, L.; Peggie, M.; Cohen, P. Use of the pharmacological inhibitor BX795 to study the regulation and physiological roles of TBK1 and IkappaB kinase epsilon: a distinct upstream kinase mediates Ser-172 phosphorylation and activation. *J. Biol. Chem.* **2009**, *284*, 14136−14146. (b) McIver, E. G.; Bryans, J.; Birchall, K.; Chugh, J.; Drake, T.; Lewis, S. J.; Osborne, J.; Smiljanic-Hurley, E.; Tsang, W.; Kamal, A.; Levy, A.; Newman, M.; Taylor, D.; Arthur, J. S. C.; Clark, K.; Cohen, P. Synthesis and structure-activity relationships of a novel series of pyrimidines as potent inhibitors of TBK1/IKKε kinases. *Bioorg. Med. Chem. Lett.* **2012**, *22*, 7169−7173. (c) Yu, T.; Yang, Y.; Yin, D. Q.; Hong, S.; Son, Y.-J.; Kim, J.-H.; Cho, J. Y. TBK1 inhibitors: a review of patent literature (2011 - 2014). *Expert Opin. Ther. Pat.* **2015**, *25*, 1385−1396.

(15) Barbie, D. A.; Tamayo, P.; Boehm, J. S.; Kim, S. Y.; Moody, S. E.; Dunn, I. F.; Schinzel, A. C.; Sandy, P.; Meylan, E.; Scholl, C.; Fröhling, S.; Chan, E. M.; Sos, M. L.; Michel, K.; Mermel, C.; Silver, S.

J.; Weir, B. A.; Reiling, J. H.; Sheng, Q.; Gupta, P. B.; Wadlow, R. C.; Le, H.; Hoersch, S.; Wittner, B. S.; Ramaswamy, S.; Livingston, D. M.; Sabatini, D. M.; Meyerson, M.; Thomas, R. K.; Lander, E. S.; Mesirov, J. P.; Root, D. E.; Gilliland, D. G.; Jacks, T.; Hahn, W. C. Systematic RNA interference reveals that oncogenic *KRAS*-driven cancers require TBK1. *Nature* **2009**, *462*, 108−112.

(16) Muvaffak, A.; Pan, Q.; Yan, H.; Fernandez, R.; Lim, J.; Dolinski, B.; Nguyen, T. T.; Strack, P.; Wu, S.; Chung, R.; Zhang, W.; Hulton, C.; Ripley, S.; Hirsch, H.; Nagashima, K.; Wong, K. K.; Jánne, P. A.; Seidel-Dugan, C.; Zawel, L.; Kirschmeier, P. T.; Middleton, R. E.; Morris, E. J.; Wang, Y. Evaluating TBK1 as a therapeutic target in cancers with activated IRF3. *Mol. Cancer Res.* **2014**, *12*, 1055−1066.

(17) Larabi, A.; Devos, J. M.; Ng, S.-L.; Nanao, M. H.; Round, A.; Maniatis, T.; Panne, D. Crystal structure and mechanism of activation of TANK-binding kinase 1. *Cell Rep.* **2013**, *3*, 734−746.

(18) Iwai, K.; Yamanaka, K.; Kamura, T.; Minato, N.; Conaway, R. C.; Conaway, J. W.; Klausner, R. D.; Pause, A. Identification of the von Hippel-Lindau tumor-suppressor protein as part of an active E3 ubiquitin ligase complex. *Proc. Natl. Acad. Sci. U. S. A.* **1999**, *96*, 12436−12441.

(19) Crews, C. M.; Buckley, D.; Ciulli, A.; Jorgensen, W.; Gareiss, P. C.; Van Molle, I.; Gustafson, J.; Tae, H.-S.; Michel, J.; Hoyer, D. W.; Roth, A. G.; Harling, J. D.; Smith, I. E. D.; Miah, A. H.; Campos, S. A.; Le, J. Compounds and Methods for the Enhanced Degradation of Targeted Proteins and Other Polypeptides by an E3 Ubiquitin Ligase, Particularly Targeting the von Hippel-Lindau E3 Ubiquitin Ligase Using Hydroxyproline Analogs to Disrupt the VHL/HIF-1$\alpha$ Interaction. WO 2013/106643, Jul 18, 2013.

(20) Galdeano, C.; Gadd, M. S.; Soares, P.; Scaffidi, S.; Van Molle, I.; Birced, I.; Hewitt, S.; Dias, D. M.; Ciulli, A. Structure-guided design and optimization of small molecules targeting the protein-protein interaction between the von Hippel-Lindau (VHL) E3 ubiquitin ligase and the hypoxia inducible factor (HIF) alpha subunit with in vitro nanomolar affinities. *J. Med. Chem.* **2014**, *57*, 8657−8663.

(21) Zengerle, M.; Chan, K.-K.; Ciulli, A. Selective small molecule induced degradation of the BET bromodomain protein BRD4. *ACS Chem. Biol.* **2015**, *10*, 1770−1777.

(22) Gadd, M. S.; Testa, A.; Lucas, X.; Chan, K.-K.; Chen, W.; Lamont, D. J.; Zengerle, M.; Ciulli, A. Structural basis of PROTAC cooperative recognition for BRD4 selective protein degradation. *Nat. Chem. Biol.* **2017**, *13*, 514−521.

(23) Hutti, J. E.; Porter, M. A.; Cheely, A. W.; Cantley, L. C.; Wang, X.; Kireev, D.; Baldwin, A. S.; Janzen, W. P. Development of a high-throughput assay for identifying inhibitors of TBK1 and IKK$\varepsilon$. *PLoS One* **2012**, *7* (7), e41494.

(24) Komander, D. The emerging complexity of protein ubiquitination. *Biochem. Soc. Trans.* **2009**, *37* (5), 937−953.



DOI: 10.1021/acs.jmedchem.7b00635
*J. Med. Chem.* 2018, 61, 583−598